Generation of Three-Dimensional Lake Model Forecasts for Lake Erie*

JOHN G. W. KELLEY AND JAY S. HOBGOOD

Atmospheric Sciences Program, Ohio State University, Columbus, Ohio

KEITH W. BEDFORD

Department of Civil and Environmental Engineering and Geodetic Science, Ohio State University, Columbus, Ohio

DAVID J. SCHWAB

Great Lakes Environmental Research Laboratory, NOAA, Ann Arbor, Michigan

(Manuscript received 8 May 1997, in final form 3 December 1997)

ABSTRACT

A one-way coupled atmospheric–lake modeling system was developed to generate short-term, mesoscale lake circulation, water level, and temperature forecasts for Lake Erie. The coupled system consisted of the semi-operational versions of the Pennsylvania State University–National Center for Atmospheric Research three-dimensional, mesoscale meteorological model (MM4), and the three-dimensional lake circulation model of the Great Lakes Forecasting System (GLFS).

The coupled system was tested using archived MM4 36-h forecasts for three cases during 1992 and 1993. The cases were chosen to demonstrate and evaluate the forecasts produced by the coupled system during severe lake conditions and at different stages in the lake's annual thermal cycle. For each case, the lake model was run for 36 h using surface heat and momentum fluxes derived from MM4's hourly meteorological forecasts and surface water temperatures from the lake model. Evaluations of the lake forecasts were conducted by comparing forecasts to observations and lake model hindcasts.

Lake temperatures were generally predicted well by the coupled system. Below the surface, the forecasts depicted the evolution of the lake's thermal structure, although not as rapidly as in the hindcasts. The greatest shortcomings were in the predictions of peak water levels and times of occurrence. The deficiencies in the lake forecasts were related primarily to wind direction errors and underestimation of surface wind speeds by the atmospheric model.

The three cases demonstrated both the potential and limitations of daily high-resolution lake forecasts for the Great Lakes. Twice daily or more frequent lake forecasts are now feasible for Lake Erie with the operational implementation of mesoscale atmospheric models such as the U.S. National Weather Service's Eta Model and Rapid Update Cycle.

1. Introduction

The Great Lakes, with a total surface area of 246 000 km², exert a strong influence on the atmosphere over the lakes and surrounding region. Numerous observational and modeling studies have demonstrated that the lakes are responsible for the development and/or intensification of atmospheric systems at a variety of spatial and temporal scales. These lake-related atmospheric systems influence the weather and climate of the region (Eichenlaub 1979) as well as the water levels, thermal structure, and circulation of the lakes (Boyce et al. 1989). Severe lake wave and storm surge conditions can result in coastal flooding and erosion, disruption of navigation, property damage, and loss of lives. Sudden changes in a lake's thermal structure can have significant impact on its chemical and biological structure (Mortimer 1987).

Several statistical techniques and numerical models have been developed to aid lake forecasters in the prediction of wave and storm surge conditions on the Great Lakes (Schwab 1978; Schwab et al. 1984). These techniques and models are used for the prediction of surface wave and storm surge conditions at selected points. However, there is a growing demand for subsurface information as well as high-resolution surface forecasts in coastal areas. This demand was recognized by the

Corresponding author address: Dr. John G. W. Kelley, Coast Survey Development Laboratory, National Ocean Service, N/CS13, Room 7875, 1315 East–West Highway, Silver Spring, MD 20910-3282.
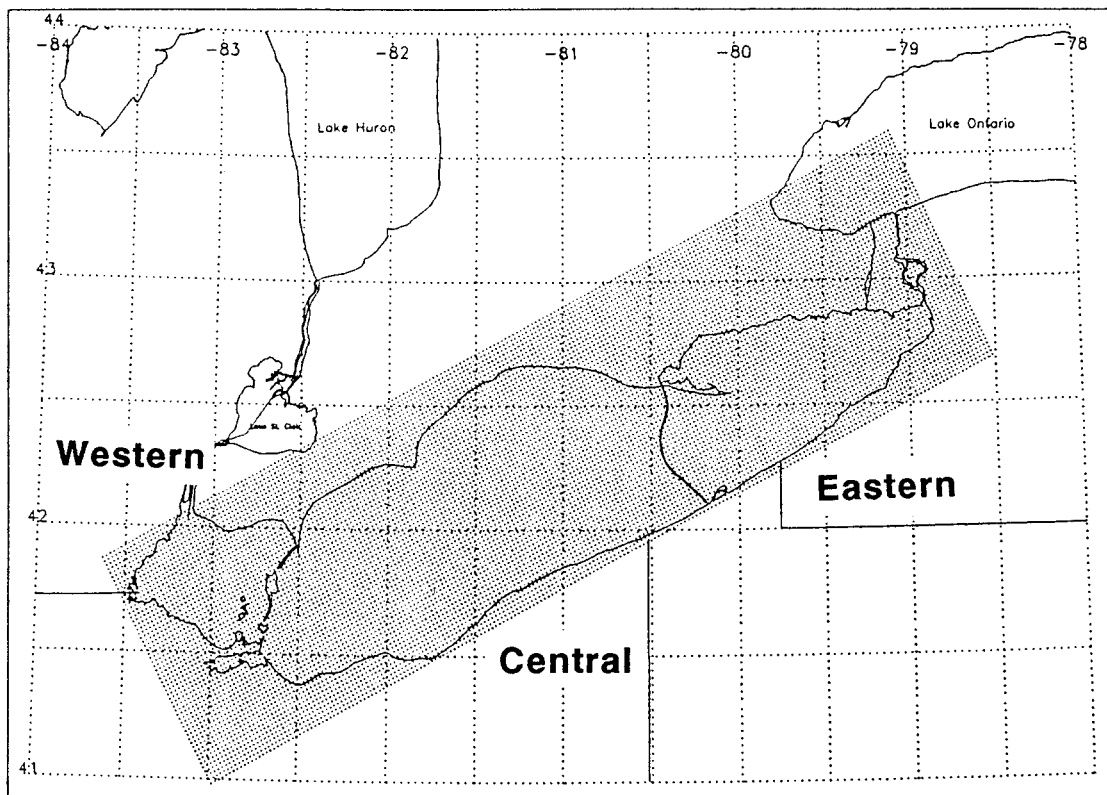E-mail: johnk@ceob.nos.noaa.gov

FIG. 1. The location of "center" grid points of the LEIFS lake model along with basin borders.

U.S. National Research Council (NRC), which recommended that the nation establish an "operational capability for nowcasting and forecasting oceanic velocity, temperature, and related fields to support coastal and offshore operations and management" (NRC 1989). Although several three-dimensional lake circulation models were developed and tested for the Great Lakes in the 1970s (Simons 1976; Bennett 1978), none were implemented operationally due to computational constraints. However, advances in computational capability and availability of real-time meteorological and limnological data in the early 1990s made it possible for the development and implementation of an operational nowcast system for Lake Erie.

The Lake Erie Information Forecast System (LEIFS) is a prototype of the Great Lakes Forecasting System (GLFS) being developed by Ohio State University (OSU) and NOAA's Great Lakes Environmental Research Laboratory (GLERL) (Schwab and Bedford 1994). The purpose of GLFS is to provide nowcasts and short-range forecasts of the physical conditions of the five Great Lakes and Lake St. Clair. The primary components of LEIFS are a three-dimensional lake circulation model and a parametric wave model. Currently, LEIFS is used to generate nowcasts for Lake Erie during the ice-free season (Yen et al. 1994). The generation of short-range lake forecasts by LEIFS will require high-

resolution predictions of overwater surface heat and momentum fluxes. Previous research by Chagnon and Jones (1972) and Lyons (1971) on the planetary boundary layer over the Great Lakes implies that an atmospheric model should have a horizontal grid resolution of approximately 25 km or less and a vertical resolution of less than 100 m near the surface to successfully simulate and predict overwater conditions. Mesoscale atmospheric prediction systems planned by the U.S. National Centers for Environmental Prediction (NCEP) and the Canadian Meteorological Center will have horizontal and vertical resolutions approaching these values.

The purpose of this study is to demonstrate and evaluate the capability to forecast surface and subsurface physical conditions for Lake Erie. This was achieved by one-way coupling the three-dimensional lake circulation model of LEIFS with an atmospheric model possessing a horizontal resolution similar to those planned for the region. The wave model of LEIFS was not used in this study. The atmospheric model chosen for this study was the semioperational version of the Pennsylvania State University–National Center for Atmospheric Research (Penn State–NCAR) mesoscale meteorological model (MM4). Three one-way coupled model runs for Lake Erie were conducted using 36-h forecasts from MM4 as input for the lake circulation model. The three cases were chosen at different stages
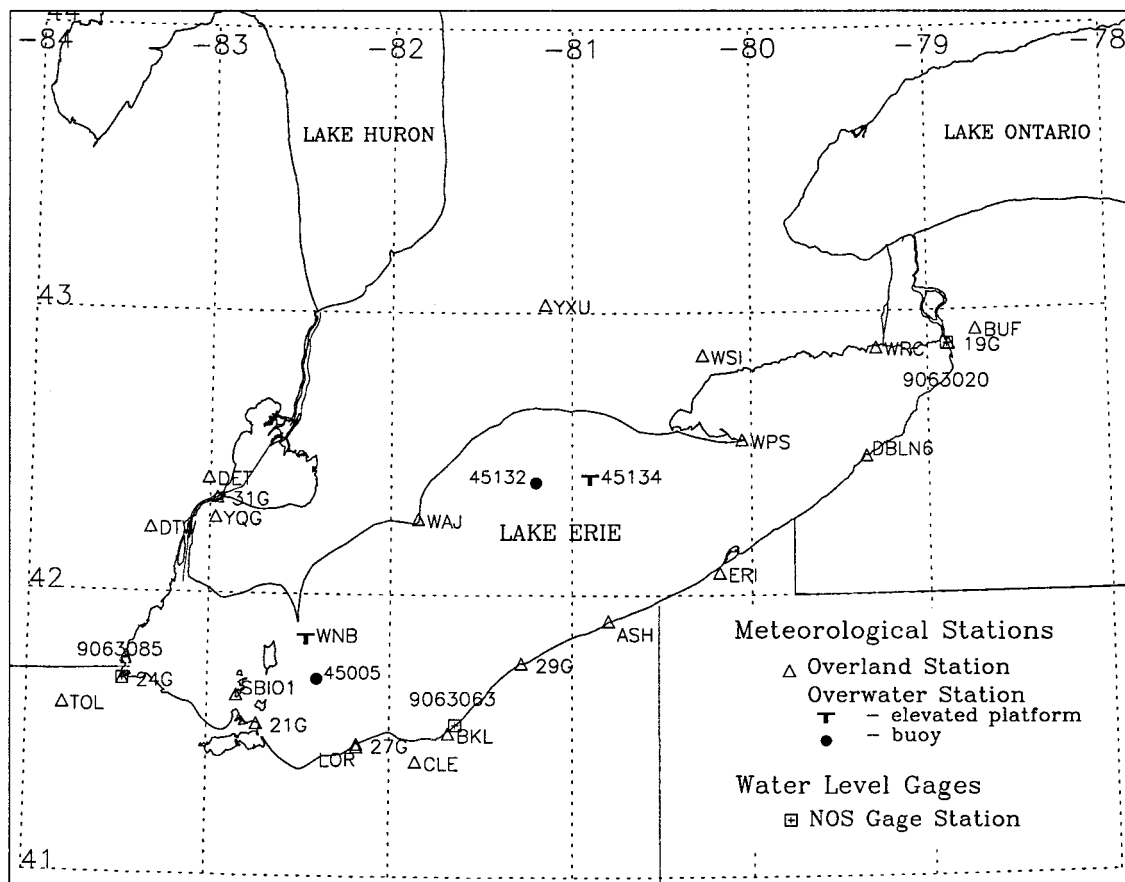
FIG. 2. Geographic locations of the U.S. NOS water level gauges and U.S. and Canadian meteorological stations.

in the annual thermal cycle of the lake and during significant storm surges and seiche activity. The lake model was also used to produce lake hindcasts for the same periods using observed data as input. The lake forecasts were compared to both the hindcasts and available surface observations with the emphasis on surface and subsurface water temperatures and water levels.

Overviews of the lake and atmospheric prediction systems are given in sections 2 and 3, respectively. A description of the methodology used to one-way couple the systems is presented in section 4. The procedure used to generate the lake forecasts as well as the methods used to evaluate lake and atmospheric forecasts are described in section 5. The three cases are discussed in sections 6–8. For each case, the lake and atmospheric conditions are described along with evaluations of MM4's meteorological and LEIFS lake forecasts. The summary and conclusions are presented in sections 9 and 10, respectively.

2. Lake prediction system

The version of LEIFS used for this study consisted of a three-dimensional lake circulation model, surface momentum and heat flux models, and an objective analysis technique. The lake circulation model is a modified version of the Princeton University three-dimensional, primitive equation, hydrostatic, coastal ocean prediction model (Blumberg and Mellor 1987; Mellor 1996). The model is commonly referred to as the Princeton Ocean Model. The model explicitly predicts three-dimensional velocity distribution, temperature, salinity, turbulent kinetic energy, turbulence macroscale, and free surface water elevation.

The model domain for Lake Erie consists of a rectangular grid with a 2-km horizontal resolution in both the x and y directions. The domain has 209 grid points in the x direction and 57 points in the y direction. The domain has been rotated so that the x coordinate is along the long axis of the lake and the y axis is across the lake (Fig. 1). The bottom topography for the domain is based on GLERL digital bathymetry data (Schwab and Sellers 1980) but smoothed by Kuan (1995) to minimize the development of numerical instability. The model uses 11 sigma levels in the vertical with levels located at 0, -0.1, -0.2, -0.3, -0.4, -0.5, -0.6, -0.7, -0.8, -0.9, and -1.0. This vertical configuration results in a maximum vertical spacing between sigma levels of ap-
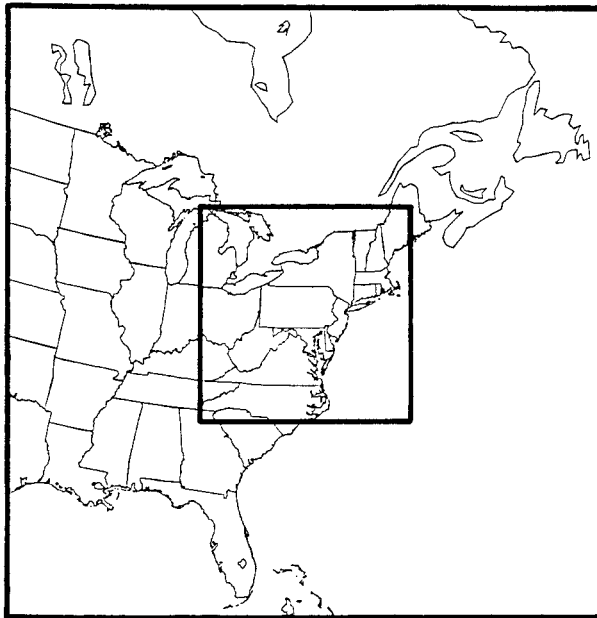
FIG. 3. The coarse- (outer border) and fine-grid (inner border) domains of the semioperational Penn State–NCAR MM4 (Warner and Seaman 1990). The horizontal resolutions of the coarse and fine grids are 90 km and 30 km.

proximately 6 m in the deepest point of the lake to 0.3 m in the shallowest locations. An internal time step of 600 s was used along with an external time step of 25 s. The lake is assumed to be completely enclosed (i.e., river inflows and outflows are considered negligible). In addition, evaporation and precipitation at the lake surface are not considered in the calculation of the water

levels. However, the mean lake water level is updated frequently by taking a weighted average of water level observations from National Ocean Service (NOS) gauges at Toledo and Cleveland, Ohio, and Buffalo, New York (Fig. 2). Additional details on the lake model can be found in Schwab and Bedford (1994) and Kelley (1995).

The surface momentum and heat flux boundary conditions for the lake model are estimated using models, gridded overlake and adjusted overland meteorological observations, and lake surface temperatures (LSTs). The surface heat flux is estimated at each grid point using the heat flux model of McCormick and Meadows (1988). The surface momentum flux is calculated at each point using a flux model developed at GLERL and OSU (Schwab 1978; Liu and Schwab 1987). In the flux model, the friction velocity for the surface drag coefficient is estimated using the profile method that takes into account air–lake temperature differences.

Overlake meteorological fields are obtained by adjusting and interpolating surface air and dewpoint temperatures, wind velocity, and cloud cover observations from both overland and overwater observing sites. Overlake sites include U.S. National Data Buoy Center (NDBC) and Canadian Atmospheric Environment Service (AES) meteorological buoys and platforms (Fig. 2). Overland sites included automated stations of the U.S. Coastal-Marine Automated Network, automated coastal stations of AES, U.S. and Canadian surface airway stations, automated stations operated by the U.S. National Weather Service Forecast Office in Cleveland, Ohio, and U.S. Coast Guard stations. Weather observations from land-based stations are adjusted to be more representative of overwater conditions. Air and dew-
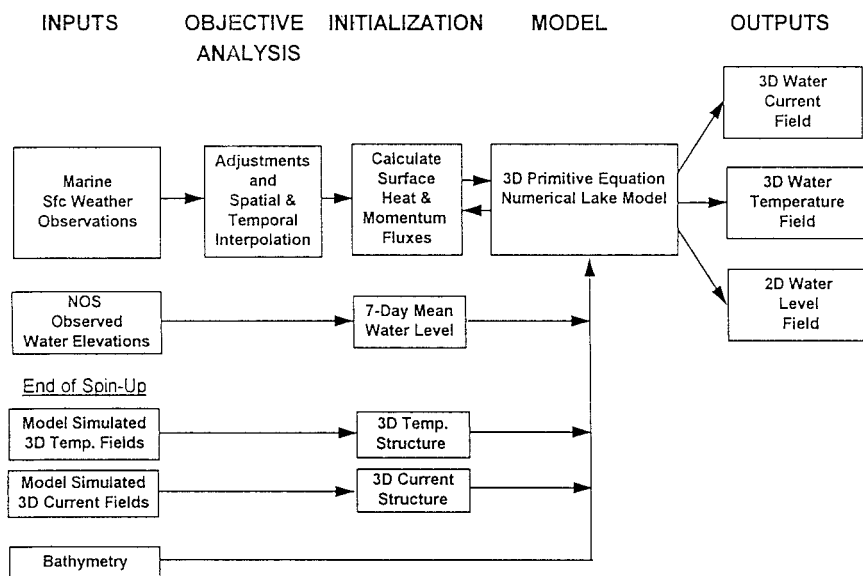

FIG. 4. Steps in the one-way coupling of MM4 with the lake model to produce short-term lake forecasts.
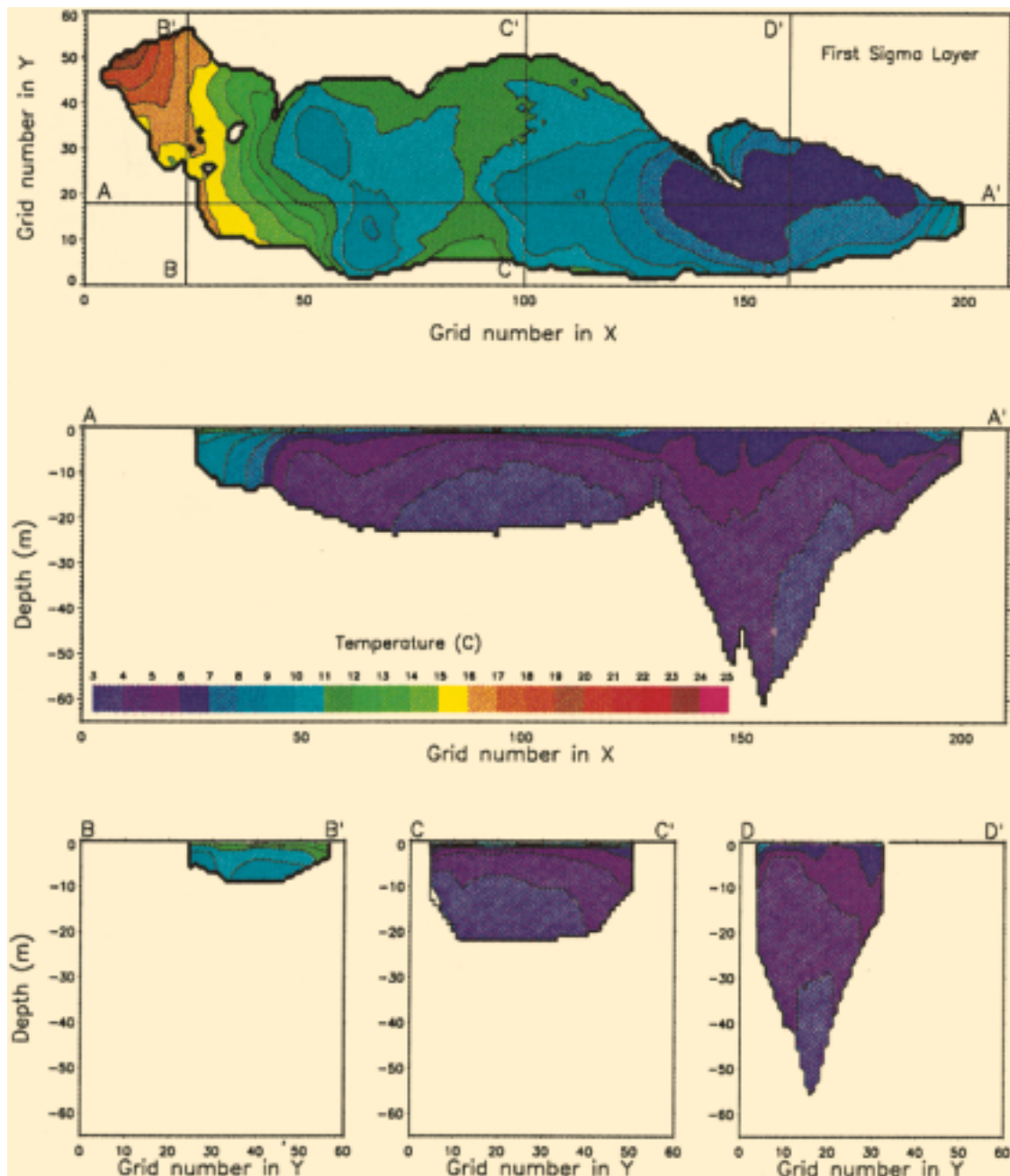
FIG. 5. LEIFS initial surface water temperatures along with long-axis and transverse vertical cross sections for 0000 UTC 12 May 1993.

point temperatures are adjusted using approximations to the data of Phillips and Irbe (1978). Wind directions from land stations are modified using an approximation to the curves of Resio and Vincent (1977) as described in Schwab (1983). Wind speeds at land stations are modified using the method of Resio and Vincent (1977). In addition, wind speed observations from all stations are adjusted to a standard measurement height of 10 m above lake level. This height was chosen since this is

an elevation sufficiently near the water surface to have a direct relationship to processes at the air–lake surface, but high enough to be above storm wave crests (Thompson and Leenknecht 1994).

3. Atmospheric modeling system

The atmospheric model used in this study is the Penn State–NCAR mesoscale meteorological modeling sys-
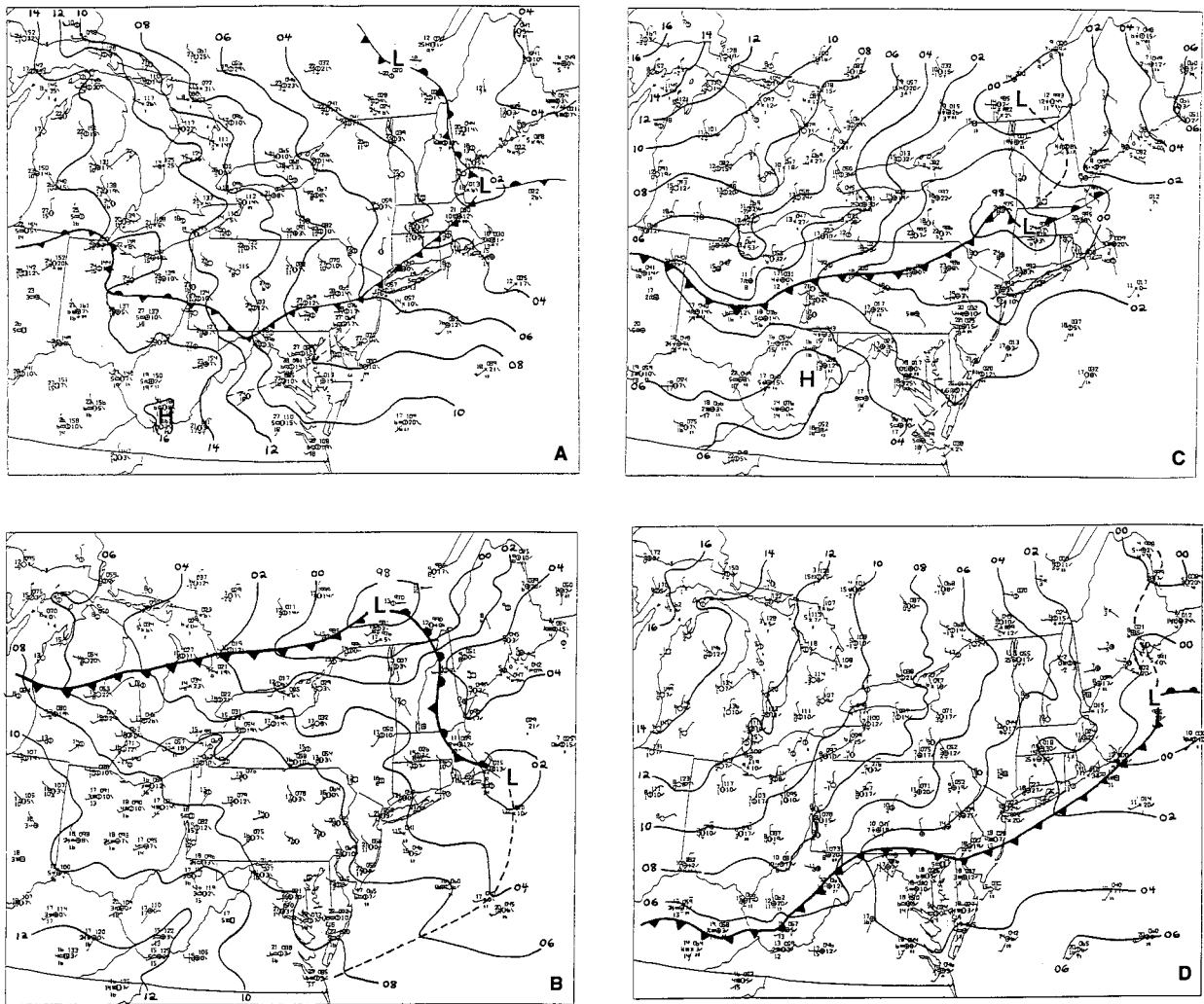
FIG. 6. Surface analyses for (a) 0000 UTC 12 May 1993, (b) 1200 UTC 12 May 1993, (c) 0000 UTC 13 May 1993, and (d) 1200 UTC 13 May 1993. Light solid lines are isobars (mb) plotted at an interval of 2 mb. Pressure troughs are noted by dashed lines.

tem. This modeling system was selected for several reasons. First, the system has been shown to simulate a variety of mesoscale meteorological features (Anthes 1990) including some features observed in the Great Lakes region (Byrd and Penc 1992; Sousounis and Fritsch 1994). Second, the modeling system has been used to produce semioperational real-time, numerical forecasts for the central (Rew 1992) and northeastern United States, including the Lake Erie region (Warner and Seaman 1990). The resolution of these forecasts is comparable to forecasts from operational models planned by U.S. and Canada meteorological forecast centers. Lastly, the modeling system has been coupled to other physical models including air pollution transport models (Hass et al. 1990), hydrologic models (Warner et al. 1991), and a one-dimensional thermal lake model (Bates et al. 1993).

For this study, archived output was obtained from the "on-call," fourth-generation version of the Penn State–

NCAR Mesoscale Model (MM4) used at Penn State to produce short-term forecasts for the northeastern United States. This configuration of the MM4 used 16 sigma levels and a singly nested, two-way interactive grid system consisting of a finer grid within a coarse grid (Fig. 3). The fine grid was a 43×43 point mesh centered over the northeastern United States with horizontal resolution of 30 km. The coarse grid was a 41×41 point mesh with a resolution of 90 km. The model used a time step of 180 s for the 90-km coarse mesh and 60 s for the 30-km fine mesh. Lateral boundary conditions were determined using analyses and 12-h forecasts from NCEP's Nested Grid Model (Hoke et al. 1989).

Planetary boundary layer (PBL) processes were parameterized using the one-dimensional, high-resolution moist PBL–surface model described by Zhang and Anthes (1982) and following Blackadar (1976, 1979). Surface water temperatures for lakes and oceans were not computed, but held constant as the model was integrated
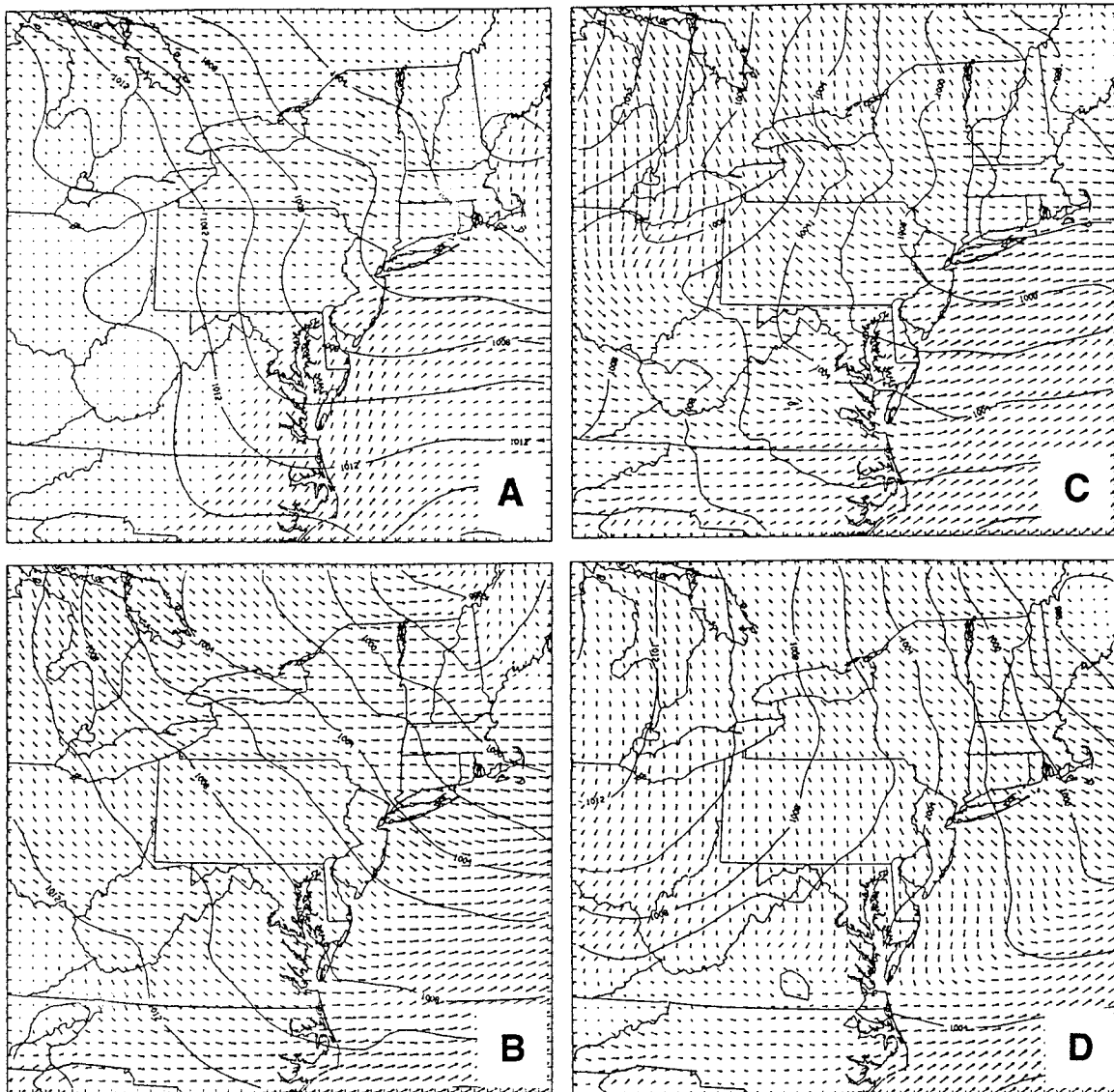
FIG. 7. MM4 fine-grid domain analysis and 12-, 24-, and 36-h forecasts of sea level pressure (mb) and surface (40 m AGL) winds (m s^{-1}) at (a) 0000 UTC 12 May 1993, (b) 1200 UTC 12 May 1993, (c) 0000 UTC 13 May 1993, and (d) 1200 UTC 13 May 1993. Light solid lines are isobars (mb) plotted at an interval of 2 mb.

forward in time. For the ocean, sea surface temperatures were estimated from the National Oceanic and Atmospheric Administration's (NOAA) 14-km experimental surface water temperature analysis updated every 6 weeks. For the Great Lakes, NOAA's LST analysis was used for Lakes Erie, Huron, and Ontario. For Lakes Michigan and Superior, the LSTs were determined in the following manner. First, the difference between NOAA's LST analysis and LST climatology was calculated for Lake Huron. Next, this difference was applied to the climatological LSTs for Lakes Superior and Michigan to estimate the LSTs (A. M. Lario-Gibbs 1994, personal communication). Specific details on the Penn State–NCAR mesoscale model can be found in

Anthes and Warner (1978), Anthes et al. (1987), and Warner and Seaman (1990).

4. Coupling of the atmospheric and lake circulation systems

The lake and atmospheric models were coupled by a mainly one-way exchange of hourly surface heat and momentum fluxes from MM4 to the lake model. Hourly surface heat and momentum fluxes could not be obtained directly from MM4 since those fluxes are not normally written out as output and archived. Instead the surface fluxes were obtained indirectly from MM4's meteorological forecasts in the following way (Fig. 4).
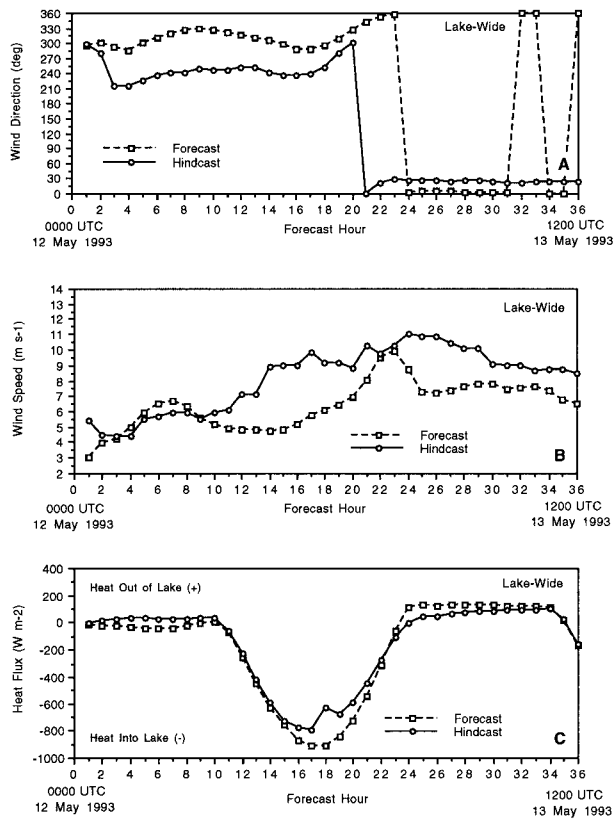
FIG. 8. Hourly lake-wide means of (a) wind direction (°), (b) wind speed (m s⁻¹), and (c) surface heat flux (W m⁻²) from 0100 UTC 12 May to 1200 UTC 13 May 1993.
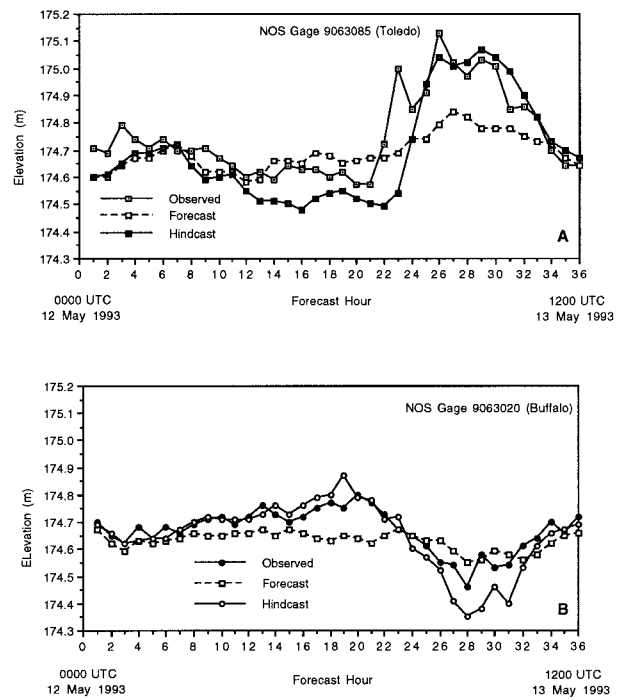

FIG. 9. Hourly forecast, hindcast, and observed water levels for NOS stations at (a) Toledo and (b) Buffalo from 0100 UTC 12 May to 1200 UTC 13 May 1993.

First, hourly MM4 forecasts of lowest prediction level (LPL) air temperature, relative humidities, and u and v wind components were interpolated to the 2-km lake model grid using the two-step Barnes interpolation scheme (Barnes 1964, 1973; Koch et al. 1983). The interpolated variables were then converted to or used to obtain those quantities required by the surface flux models. The LPL winds were extrapolated to a standard 10-m height above ground level (AGL) using the profile method mentioned earlier. Stability conditions for the method were determined using MM4's air temperature and the lake model's LST. The LPL air temperature and relative humidities were used to calculate dewpoint temperatures. No height adjustment was made to the LPL

temperatures. Hourly cloud cover was estimated using MM4's 850- and 700-mb relative humidities and a simple cloudiness–relative humidity parameterization scheme (Ricketts 1973; Sullivan 1988). Finally, the hourly MM4 forecasts were used in the flux models along with the lake model's LST prediction at the previous time step to calculate surface and momentum fluxes at each grid point.

5. Generation and evaluation of coupled forecasts

Three cases were chosen to demonstrate and evaluate forecasts produced by the coupled modeling system during severe lake conditions at different stages in the annual thermal cycle of Lake Erie. The specific criteria used in the selection of the case study periods were the following: 1) occurrence of significant storm surge and seiche activity, 2) availability of archived MM4 36-h

TABLE 1. Performance measures of hourly lake-wide mean wind and surface heat flux forecasts.

Case	Wind direction (°)			Wind speed (m s⁻¹)			Surface heat flux (W m⁻²)		
	Mean diff. (F − O)	Mean absol. diff.	Index of agreement	Mean diff. (F − O)	Mean absol. diff.	Index of agreement	Mean diff. (F − O)	Mean absol. diff.	Index of agreement
Spring	22.3	42.6	—	−1.7	1.9	0.70	112.6	121.3	0.94
Summer	4.1	23.4	—	−4.9	4.9	0.35	−167.1	167.1	0.80
Autumn	7.3	13.4	—	−0.9	2.3	0.83	2.7	178.3	0.92

TABLE 2. Performance measures of extreme water level forecasts and hindcasts.

		Maximum water level				Minimum water level			
		Amplitude		Phase		Amplitude		Phase	
Case	Type	Diff. (F − O) (m)	Score	Diff. (F − O) (h)	Score	Diff. (F − O) (m)	Score	Diff. (F − O) (h)	Score
Spring	Fcst	−0.29	0.5	1	0.8	0.09	0.9	0	1.0
	Hcst	−0.06	0.9	3	0.4	−0.11	0.8	0	1.0
Summer	Fcst	−0.54	0.0	11	0.0	0.39	0.3	−9	0.0
	Hcst	0.00	1.0	1	0.8	0.12	0.8	0	1.0
Autumn	Fcst	−0.47	0.1	6	0.0	0.42	0.2	1	0.8
	Hcst	−0.16	0.7	2	0.6	−0.23	0.6	−1	0.9

forecast output, and 3) at least one case for spring, summer, and autumn. Using these criteria, the following three cases were selected: 1) 12–13 May 1993, 2) 30 July–1 August 1992, and 3) 16–18 October 1992.

The three-dimensional structure or ''initial'' conditions at the beginning of each case could not be specified from observed data due to the lack of operational subsurface temperature and current data in the Great Lakes. Instead the lake model was spun up for 2 weeks prior to each case study using surface fluxes derived from observed meteorological data. The three-dimensional thermal and current structure at the start of each spinup period was accomplished in the following manner. The three-dimensional current field was set to zero. Thermal structure was defined using a 5-day mean satellite-derived LST composite and a vertical water temperature profile representative of the case study date. The composite was generated using daily LST fields estimated from daytime imagery data from the Advanced Very High Resolution Radiometer onboard the *NOAA-11* polar-orbiting satellite. The top and bottom layers were considered isothermal with grid points in the top layer assigned temperatures equal to the LST and bottom layer grid points assigned to 5°C. The middle layer was defined as a zone of linearly decreasing temperatures. The depth of the middle layer was estimated based on the seasonal profiles of Schertzer et al. (1987). Schertzer's profiles have been used previously by O'Connor and Schwab (1993) for specifying the initial thermal structure of the lake.

After the 2-week spinup, the lake model was run for 36 h using archived MM4 forecasts and the coupling procedure discussed in the previous section. The resultant lake forecasts were evaluated both on a lake-wide basis and for some variables at specific points on the lake. In the absence of measurements from in situ or space-based remote sensors, the forecasts were compared spatially against model hindcasts generated for the forecast period using the same initial lake conditions but fluxes derived from observed meteorological conditions. These hindcasts provided an estimate of the actual three-dimensional structure of the lake. The lake model's ability to accurately simulate Lake Erie's water

levels and thermal and circulation structure has been previously demonstrated by Kuan (1995).

The point evaluations were made by comparing LST and water level forecasts to observations from NDBC fixed buoy 45005 and AES fixed buoy 45132 and platform 45134 and NOS water level gauges at Toledo and Buffalo (Fig. 2). The depth of the model LST forecasts was between 0.6 and 1.1 m, similar to the 0.5-m depth of the observations (Gilhousen 1987). The LST forecasts at buoy 45005 were also evaluated in terms of relative performance by comparing the predictions against an hourly LST climatology. Comparisons between lake forecasts, hindcasts, climatology, and observations were done using graphical techniques and statistical measures. These statistical measures included two absolute quantities, mean algebraic and absolute differences, one relative quantity, the index of agreement (IOA) (Willmott 1984), and two skill tests. IOA is a measure of the degree to which a model's predictions are error free. It is considered an alternative to the correlation coefficient, which suffers from its inability to discern differences in proportionality and/or constant additive differences between the two variables (Willmott 1982). The two skill tests included the peak amplitude skill and the phase tests (Dingman and Bedford 1986). The amplitude skill test was used to determine the ability of the model to forecast the maximum and minimum water levels at opposite ends of the lake. An arbitrary scoring method was used to assign a specific number of points based on the absolute difference between the forecast and observed water levels. A score of 1.0 is assigned if the difference is less than 0.05 m. The phase test is used to judge the ability of the model to forecast the time of occurrence of the extreme water levels. A time difference of 0 h is given a score of 1.0. Following Dingman and Bedford (1986), early forecasts of the time of occurrence received a higher score than a late prediction.

The meteorological predictions were evaluated by comparing MM4 sea level pressure (SLP) and LPL wind vector forecast maps against subjective surface analyses and to observations on a lake-wide and an individual basin scale. Due to the cyclical nature of wind direction
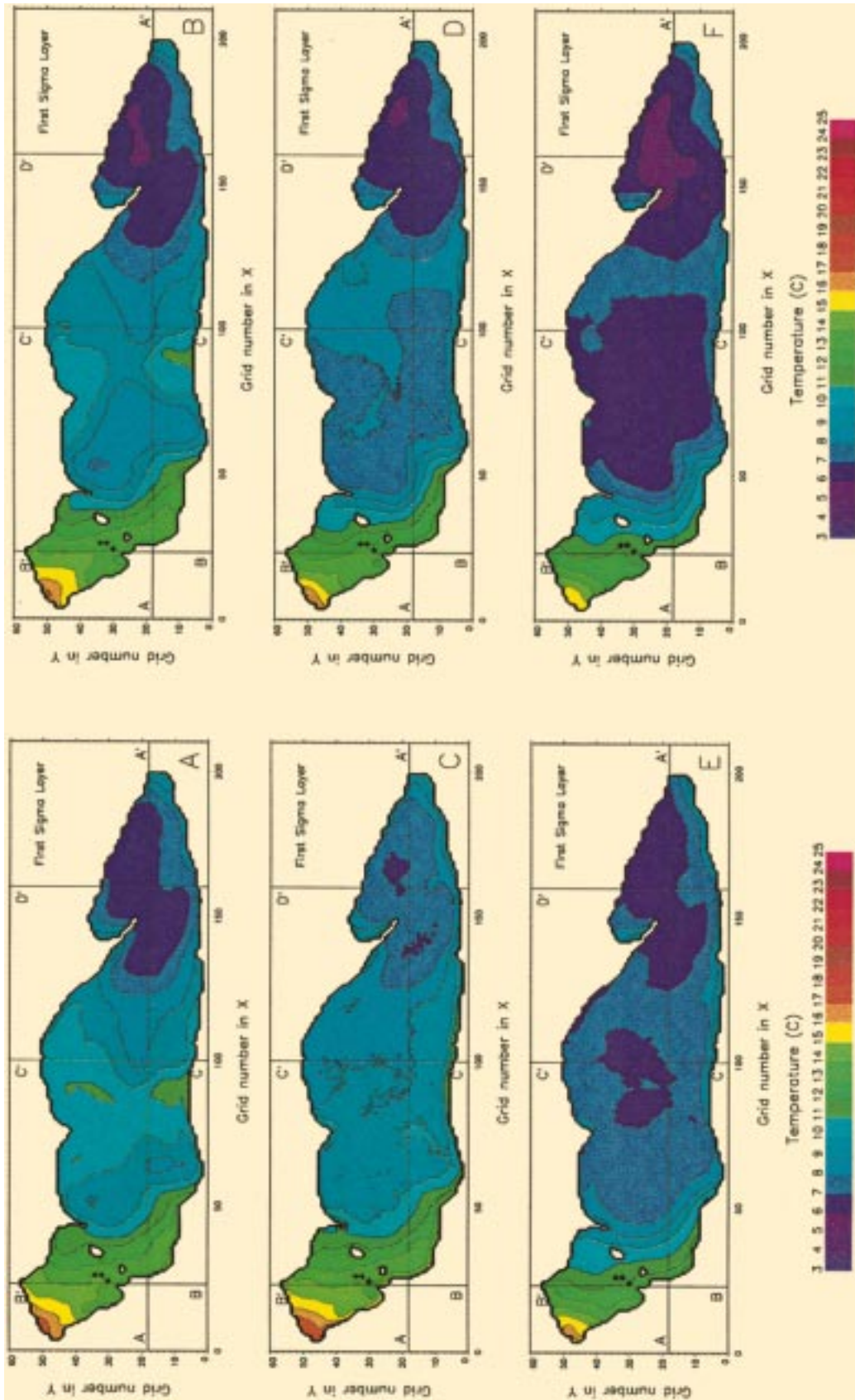
FIG. 10. LEIFS 12-, 24-, and 36-h subsurface water temperature forecasts for (a) 1200 UTC 12 May 1993, (c) 0000 UTC 13 May 1993, and (e) 1200 UTC 13 May 1993. Also shown are 12- (b), 24- (d), and 36-h (f) hindcasts for the same times. Contours are drawn at intervals of 1°C.
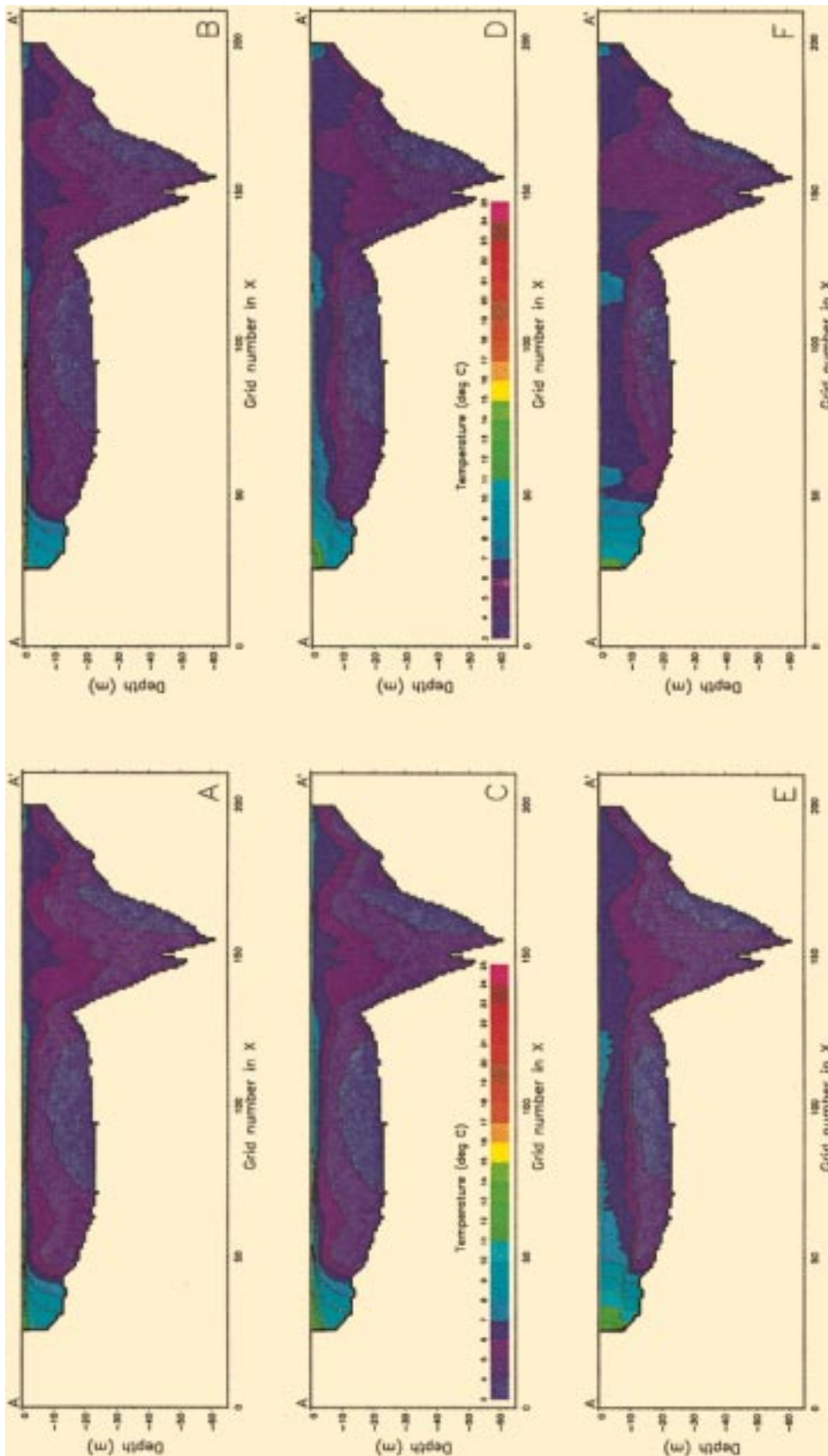
FIG. 11. LEIFS 12-, 24-, and 36-h subsurface water temperature forecasts as depicted in long-axis cross sections for (a) 1200 UTC 12 May 1993, (c) 0000 UTC 13 May 1993, and (e) 1200 UTC 13 May 1993. Also shown are 12- (b), 24- (d), and 36-h (f) hindcasts for the same times. Contours are drawn at intervals of 1°C.

TABLE 3. Performance measures of hourly surface water temperature forecasts, hindcasts, and climatology.

Case	Type of prediction	Temp (°C)								
		Buoy 45005			Buoy 43132			Platform 45134		
		Mean diff. (F − O)	Mean absol. diff.	Index of agreement	Mean diff. (F − O)	Mean absol. diff.	Index of agreement	Mean diff. (F − O)	Mean absol. diff.	Index of agreement
Spring										
	Forecast	—	—	—	0.3	0.8	0.83	−0.2	0.7	0.59
	Hindcast	—	—	—	−0.5	0.5	0.94	−0.7	0.7	0.59
	Climatology	—	—	—	—	—	—	—	—	—
Summer										
	Forecast	−0.4	0.6	0.33	0.4	0.4	0.64	−1.2	1.2	0.31
	Hindcast	−1.0	1.0	0.47	0.0	0.2	0.91	−1.8	1.8	0.23
	Climatology	3.0	3.0	0.18	—	—	—	—	—	—
Autumn										
	Forecast	0.9	0.9	0.62	—	—	—	−0.1	0.3	0.84
	Hindcast	0.6	0.6	0.76	—	—	—	−0.2	0.3	0.81
	Climatology	0.7	0.7	0.53	—	—	—	—	—	—

data (DeYoung and Tang 1989), IOA could not be used in the evaluation of the wind direction forecasts. For the mean algebraic difference, the convention of Strub and James (1990) was used in which negative values indicate wind direction forecasts to the "left" or counterclockwise of the observations while positive values indicate forecasts to the "right" or clockwise of the observations. Lake-wide and basin means were calcu-

lated for each hour for MM4's LPL forecasts of air temperature, wind direction, and wind speed (adjusted to 10 m AGL) and also for the estimated surface heat and momentum fluxes. Similarly, lakewide and basin means were calculated for the adjusted meteorological observations. Lakewide and basin means were also calculated for the surface fluxes estimated from the adjusted observations and lake model hindcasts of surface water temperatures. Only the lake-wide means are discussed in this paper.

6. Spring case

The first case study covered the period from 0000 UTC 12 May to 1200 UTC 13 May 1993. During this case, a cold front moved southward from Canada when the lake was developing a stable stratification. Detailed descriptions of the initial conditions, the atmospheric conditions during the 36-h forecast period, and evaluations of the atmospheric and lake forecasts are presented in the following sections.

a. Initial lake conditions

The lake thermal structure at the start of the period exhibited a springtime condition of "fragile" stability (Fig. 5); a situation that occurs when a shallow surface layer of warm water overlies cold water below (Schertzer et al. 1987). This is a common spring phenomena in lakes during periods of relatively calm and warm weather (Wetzel 1983). For this particular case, transverse and major-axis cross sections showed a 1–3-m-thick surface layer of warm water ranging from 12° to 20°C in the western basin to 7°–16°C in the central basin. Below this layer, temperatures were mainly 3°–7°C, except for areas of 7°–11°C in the western basin and the extreme western part of the central basin.
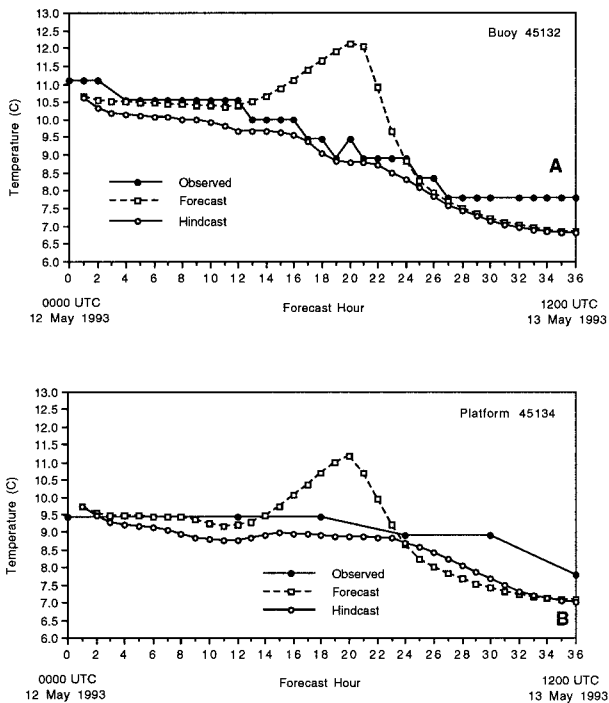

FIG. 12. Forecast, hindcast, and observed surface water temperatures for (a) buoy 45132 and (b) platform 45134 for the period 0000 UTC 12 May to 1200 UTC 13 May 1993. Observations were not available at buoy 45005.

b. Lake and atmospheric conditions

At the start of the forecast period (0000 UTC 12 May), a weak surface high was located in southern West Virginia (Fig. 6a) with overlake winds generally from the north. By 1200 UTC, the surface cyclone over Quebec had deepened and its associated cold front had moved to southern Lake Huron (Fig. 6b). In advance of the front, winds had become southwest at 5 m s⁻¹ over most of the lake. For the next 10 h, winds continued from the southwest and increased to sustained speeds of 7.7–12.8 m s⁻¹. These southwest winds resulted in a tilted water surface with a high water level at Buffalo of 174.80 m at 1900 UTC, 1.3 m above low water datum. During this period LSTs began to decrease across the lake. By 0000 UTC 13 May the cold front had passed to the south of the lake and was located over central Ohio and Pennsylvania (Fig. 6c). Winds had shifted to the north or northeast over the entire lake with sustained speeds of 7.7–10.2 m s⁻¹. At 0500 UTC the tilt in the water surface had reversed with a high water level at Toledo, Ohio, of 175.13 m, 1.63 m above datum. This was 10 h after the peak water level at Buffalo. By the end of the forecast period overlake winds were generally from the northeast at 7.7 m s⁻¹ (Fig. 6d). Observed LSTs in the central basin dropped to 7.8°C, a 3.4°C decrease in 36 h.

c. Atmospheric forecasts

A comparison of the 12-h MM4 sea level pressure and surface wind (LPL) forecasts (Fig. 7) with the surface analyses indicates that the model was successful in reproducing the location of major mesoscale features. However, it was deficient in predicting the development of southwest winds across the lake and surrounding areas prior to the cold frontal passage and northeast winds following the front. Hourly wind direction forecasts were generally from the west-northwest during the first 20 h while the actual winds were from the west-southwest (Fig. 8a). The forecast did well in the timing of the wind shift at 2000 UTC over most of the lake. For the entire 36 h, the mean algebraic difference was 22.3° clockwise from the observations. Surface wind speeds were underestimated during most of the forecast period (Fig. 8b) by approximately 2 m s⁻¹ (Table 1).

A comparison of hourly total surface heat flux forecasts versus those estimated from meteorological observations indicates an overestimation of heat into the lake by approximately 113 W m⁻² (Table 1). The greatest overestimation occurred during the daylight hours from approximately 1400 UTC to 2200 UTC 12 May (Fig. 8c). An examination of the individual heat flux components (not shown) indicates that the overestimation of heat into the lake was primarily due to a positive bias of 100–300 W m⁻² in the shortwave radiation flux forecasts. The cause for this bias was determined by examining hourly lake-wide means of the

meteorological variables used in the calculation of the fluxes (not shown). The primary reason for the overestimation was an underprediction of cloud cover by 2–6 oktas.

d. Lake forecasts

Water level forecasts (not shown) indicated a uniformly flat surface up to 0000 UTC 13 May. The model then predicted a slight "tilt" from 0000 to 0800 UTC 13 May due to the forecast of the northerly winds following the predicted frontal passage at 0000 UTC. The tilt involved a rise of the surface in the western basin and a sink or "drawdown" in the eastern basin. Hindcasts for the same period (not shown) depicted two opposite tilts during the forecast period. Between 1200 and 2000 UTC a tilt occurred with a rise of water levels in the eastern basin and a drawdown in the western basin. This was in response to the southwest winds in advance of the front. Following the passage of the cold front at 2200 UTC, northeast winds created an opposite and more pronounced tilt. Comparisons of hourly water level forecasts to observations at the three NOS gauges indicated that the forecasts provided reasonable estimates of the maximum and minimum observed water levels and their times of occurrence (Fig. 9). The forecasts underestimated the minimum water level at Buffalo by only 0.09 m and at the correct hour (Table 2). The maximum water level forecast at Toledo was underestimated by 0.29 m and 1 h late.

Forecasts of LSTs indicated a slight lake-wide cooling for the first 12 h (Fig. 10a) followed by a warming period until 2000 UTC during which the lake-wide mean rose 1.6°C. Below the surface, temperatures were forecast to remain fairly constant (Fig. 11a). Hindcasts for the same period depicted instead a gradual cooling of the LSTs (Fig. 10b) but showed a similar subsurface temperature structure (Fig. 11b). The difference in the LSTs was primarily due to the overprediction of heat flux into the lake during the daylight hours. Starting 2200 UTC 12 May, LSTs were forecast to decrease following the cold front passage (Figs. 10c and 10e). Below the surface, the forecast depicted the development of weak stratification in the central basin with an accompanying deepening of the epilimnion (upper layer of water) (Figs. 11c and 11e). Similar epilimnion deepening due to mixing by moderate wind impulses in spring have been discussed by Wetzel (1983) and Schertzer et al. (1987). Hindcasts for this period continued the cooling of LSTs (Figs. 10d and 10f). The mean lake LST lowered to 7.6°C, a drop of 2.6°C, 0.4°C cooler than the forecast decrease. Below the surface, the hindcasts supported the forecasts in the development of weak stable stratification in the central basin (Figs. 11d and 11f). However, the hindcasts depicted a more compact hypolimnion (lowest layer of water) in the central basin, a smaller vertical temperature gradient in the metalimnion (layer of thermal discontinuity between

epilimnion and hypolimnion) and a more uniform epilimnion. In the other basins, the hindcast indicated a deeper intrusion of the 5°–6°C water in the eastern basin and more isothermal conditions in the western basin. Comparisons of LSTs at buoy 45132 and platform 45134 (Table 3) indicate that the mean differences between forecasts and observations were similar to the differences between hindcasts and observations. However, hourly comparisons at buoy 45132 and platform 45134 (Fig. 12) indicate that the forecasts deviated from the observations by 1.0°–3.0°C while hindcasts varied by 0.5°–1.0°C from observations during the 36-h period. The greatest departure coincided with the period of shortwave overprediction described earlier.

7. Summer case

The second case study was for the period from 1200 UTC 30 July to 0000 UTC 1 August 1992. In this summertime case, an unseasonably intense cyclone traveled along the long axis of the lake, which was stably stratified in its central and eastern basins. The track resulted in a unique mesoscale wind field, which had a significant impact on the lake's physical structure.

a. Initial lake conditions

The initial water temperature structure was typical for late July (Mortimer 1987; Schertzer et al. 1987). At the surface, LSTs ranged from 21°–24°C in the shallow western basin to 17°–18°C in the eastern basin (Fig. 13). Below the surface, nearly isothermal conditions existed in the western basin with stable stratification in the central and eastern basins. The well-mixed western basin is a normal condition due to its shallowness and wind exposure (Mortimer 1987). In the central basin, the stratified structure consisted of an approximate 10-m-deep epilimnion with temperatures between 17° and 19°C, and a hypolimnion of about 10 m with temperatures of 13°–15°C. In the eastern basin, the stratified structure was marked by a ''doming'' of the isotherms, a thick metalimnion of 15–20 m, and a hypolimnion of 6°–8°C. The doming effect may be associated with a counterclockwise circulation in the epilimnion (Mortimer 1987; Schwab et al. 1995). The model depicted at 1200 UTC 30 July a counterclockwise gyre in the eastern basin (not shown).

b. Lake and atmospheric conditions

At the start of the forecast period, a stationary front stretched from the low through northern Ohio and central Pennsylvania and a weak 1018-mb anticyclone was centered over south Ontario (Fig. 14a). Overwater winds were from the east-northeast at 5.1–7.7 m s^{-1}. By 0000 UTC 31 July, a surface cyclone was in western Indiana (not shown) and the surface high had moved slightly to the east (Fig. 14b). Overlake winds, which during the previous 12 h had been from the east or northeast, were now from the northeast at 13 m s^{-1}. These northeast winds caused water levels at Toledo, Ohio, to rise 0.3 m between 1600 and 2200 UTC, reaching a maximum at 0200 UTC 31 July with a reading of 175.05 m, 1.55 m above datum. Five hours later the lowest water level occurred at Buffalo, New York, with a reading of 173.89 m, 0.39 m above datum. The difference between these high and low water levels represented a ''set-up'' of 1.16 m. By 1200 UTC the surface cyclone with a central pressure of 1006 mb was located over the lake between the western and central basins (Fig. 14c). A cold front extended from this low into western Ohio and southeastern Indiana while a warm front stretched over the lake northward to Ashtabula, Ohio. The positions of these fronts resulted in a complex wind field over the lake. In the western basin winds were from the north while in the central and eastern basins the winds remained from the northeast in the region north of the warm front, and southwest in areas to the south of the front. Winds shifted to the north and northeast in central and eastern basins during the next 6 h as the surface low moved northeastward. By 0000 UTC 1 August the surface low was located near the eastern shore of Lake Ontario (Fig. 14d) and overlake winds remained from the north.

c. Atmospheric forecasts

A comparison of the forecasts (Fig. 15) with the surface analyses indicate that MM4 exhibited several problems in the prediction of the surface cyclone. First, MM4 predicted that the primary cyclone would become stationary along the Ohio–Indiana border at 0600 UTC 31 (not shown) while a secondary surface low pressure area would form over the western basin and move northeastward. However, the surface analyses indicated that primary cyclone did not remain stationary and that a secondary low did not form over the lake. The other problems were that MM4 underpredicted the intensity of the low as it passed over the lake and overpredicted its forward speed. MM4 was approximately 6–8 h too fast in the forward speed of the low and overestimated the central pressure of the low by 2–4 mb; the greatest departure occurring while the low was in the vicinity of the lake. For example, the surface analysis at 1200 UTC 31 July (Fig. 14c) depicted the low in the western basin with a central pressure of 1006 mb. MM4 predicted that the low would be south of Buffalo, New York, with central pressure of 1008 mb (Fig. 15c). These problems resulted in three errors in overlake wind conditions: 1) a premature development of southwest winds in the western basin at the start of the period, 2) an underestimation of the overlake wind speeds as the low moved across the lake, and 3) a premature development of northeast winds over the entire lake starting at 1200 UTC 31 July. These errors appear in the lake-wide hourly wind direction forecasts as a shift to the northeast at
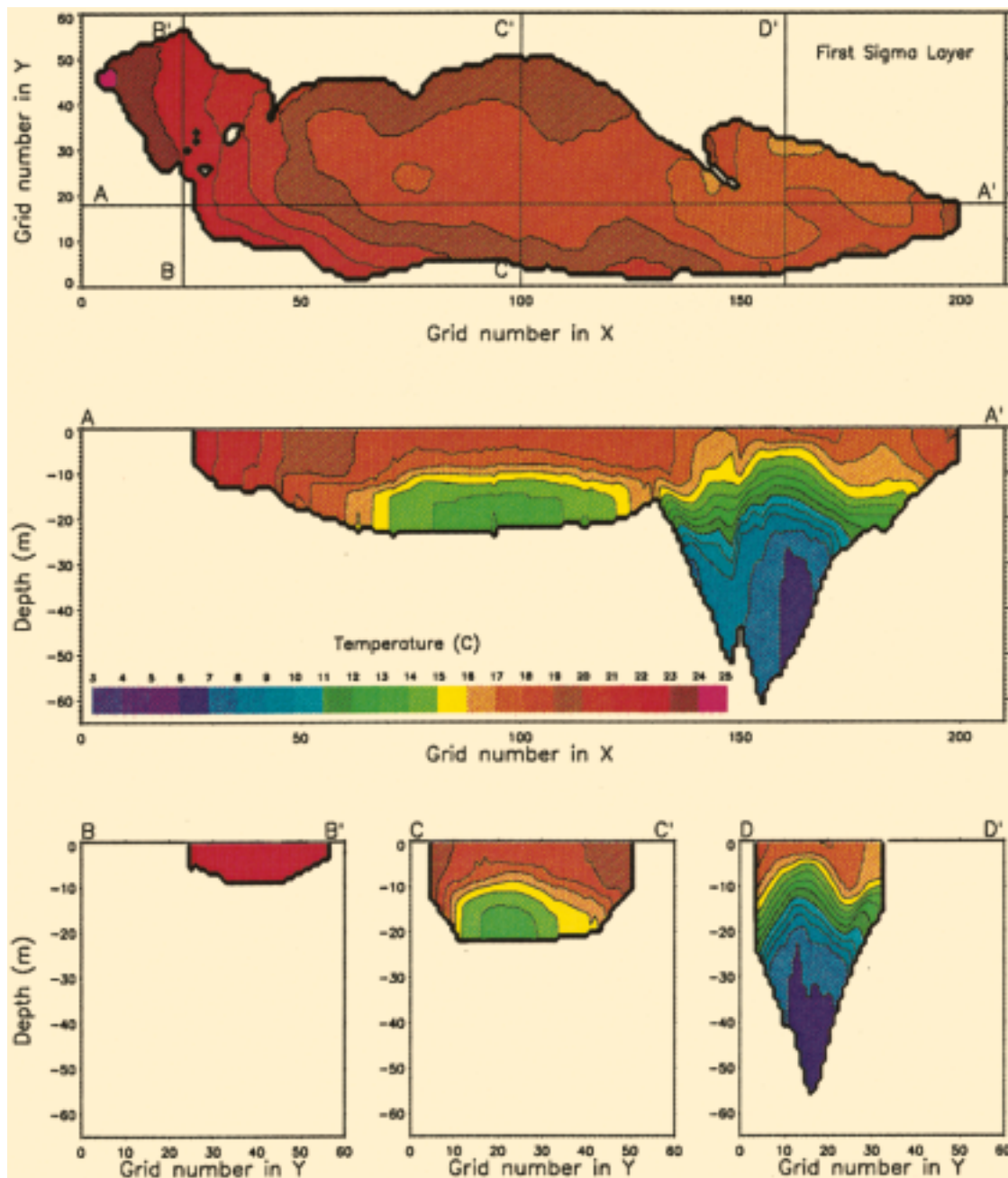
FIG. 13. LEIFS initial surface water temperatures along with long-axis and transverse vertical cross sections for 1200 UTC 30 July 1992.

1900 UTC, approximately 9 h too early (Fig. 16a). Lake-wide wind speed forecasts were approximately 5 m s^{-1} (Table 1) too low during the entire 36-h period (Fig. 16b).

Hourly forecasts of total surface heat flux overestimated the amount of heat into the lake during the daylight hours and slightly underestimated the amount of heat out of the lake at night (Fig. 16c). For the entire 36 h the absolute difference between forecasts and ob-servations was 167 W m^{-2} (Table 1). An examination of the individual components (not shown) indicated that the daytime forecast bias was due primarily to an 100–300 W m^{-2} overestimation of the shortwave radiation. This was the same reason as in the springtime case and was caused by an underestimation of the cloud cover by 2–3 oktas (not shown). The nighttime underestimation of heat loss from the lake was due to an underprediction of the latent heat flux by 50–100 W m^{-2}
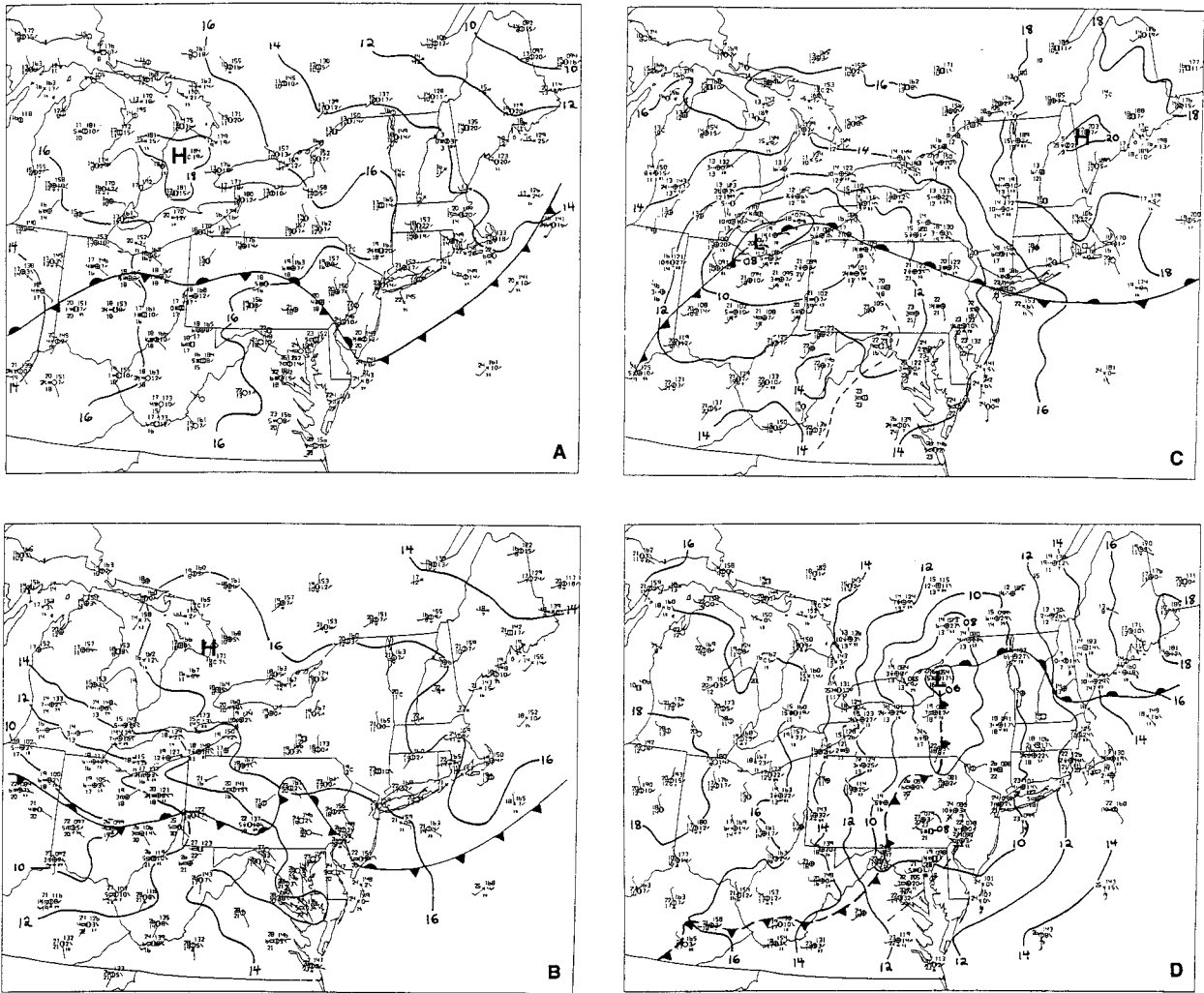
Fig. 14. Surface analyses for (a) 1200 UTC 30 July 1992, (b) 0000 UTC 31 July 1992, (c) 1200 UTC 31 July 1992, and (d) 0000 UTC 1 August 1992. Light solid lines are isobars (mb) plotted at an interval of 2 mb. Pressure troughs are noted by dashed lines.

(i.e., too little heat out of the lake by evaporation). This latent heat bias was present for all 36 h and was due to the underestimation of surface wind speeds.

d. Lake forecasts

Water level forecasts indicated a slight northeast to southwest tilt of the water surface from 2200 UTC 30 July to 1600 UTC 31 July (not shown) as winds increased from the northeast. Hindcasts for the same period depicted a more amplified tilt from 1800 UTC 30 July to 2000 UTC 31 July. Comparisons of hourly water level forecasts at the three NOS gauges indicate that the forecasts estimated poorly the extreme water levels at the opposite ends of the lake (Fig. 17). The forecast underestimated the maximum at Toledo by 0.54 m and was 11 h too late (Table 2). The minimum water level at Buffalo was underforecast by 0.39 m and was 9 h too early. The poor performance was related to the un-

derestimation of surface winds speeds and errors in the wind direction forecasts.

The forecasts of LSTs for the first 12 h called for a slight increase (Fig. 18a). Below the surface, the temperature structure was forecast to remain relatively constant in the central and western basins (Fig. 19a). However, in the eastern basin the dome was expected to become slightly more pronounced reflecting the strengthening of the counterclockwise gyre in the eastern basin. The hindcasts indicated that the LSTs would remain about constant (Fig. 18b) unlike the forecasts that indicated an increase due to the overestimation of heat into the lake (Fig. 16c). Below the surface, the hindcasts depicted a more rapid increase of the eastern basin dome along with a more compact metalimnion (Fig. 19b). The forecasts for the last 24 h (Figs. 18c and 18e) indicated a warming of LSTs, especially in the eastern and central basins. This warming was due to MM4's underestimation of heat loss from the lake at
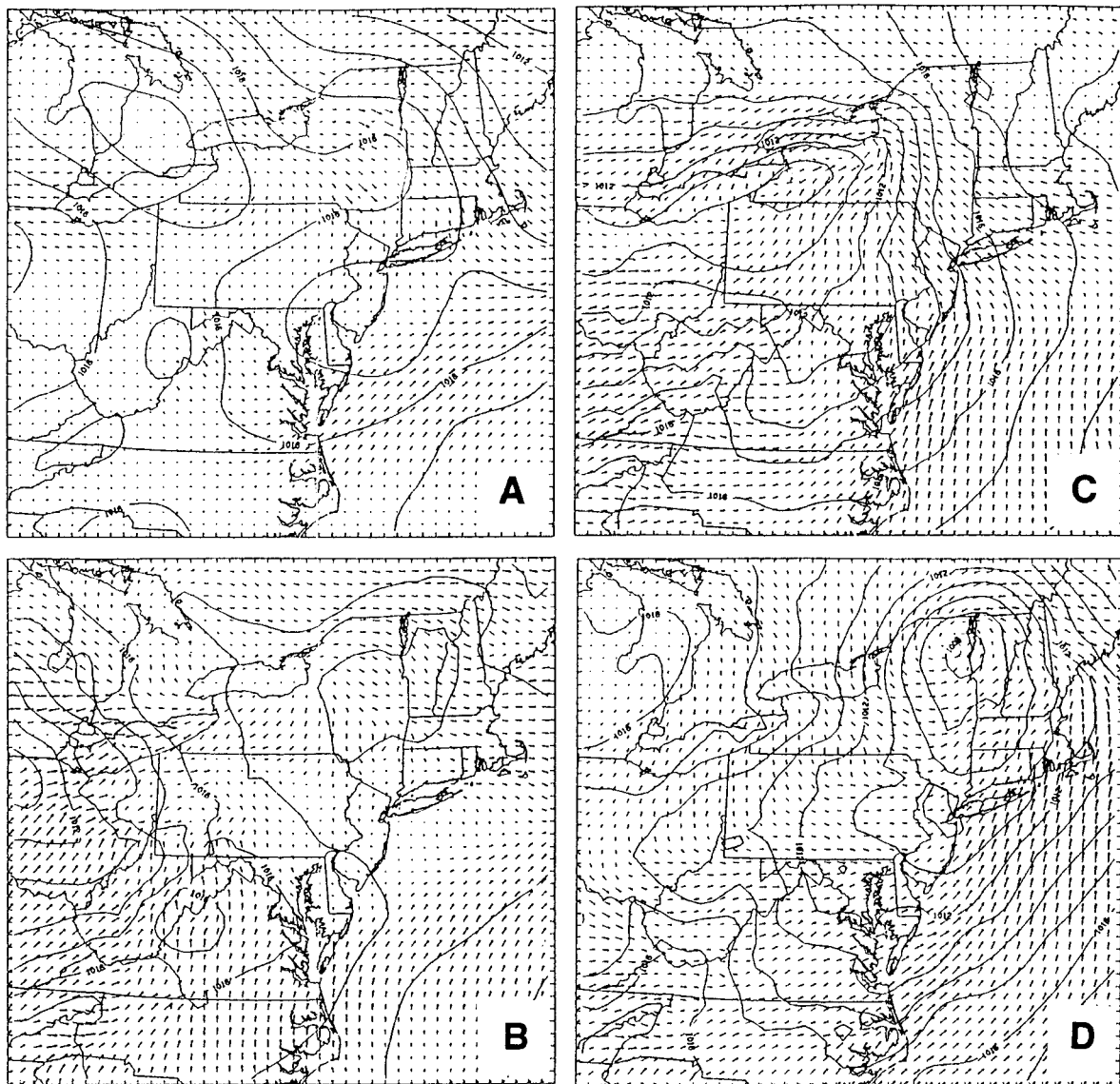
FIG. 15. MM4 fine-grid domain analysis and 12-, 24-, and 36-h forecasts of sea level pressure (mb) and surface (40 m AGL) winds (m s^{-1}) at (a) 1200 UTC 30 July 1992, (b) 0000 UTC 31 July 1992, (c) 1200 UTC 31 July 1992, and (d) 0000 UTC 1 August 1992. Light solid lines are isobars (mb) plotted at an interval of 2 mb.

night and overestimation of heat gain into the lake during the daytime (Fig. 16c). Below the surface, the doming was forecast to amplify very slightly (Figs. 19c and 19e). Elsewhere in the lake, the thermal structure was to remain the same. However, the hindcasts (Figs. 18d and 18f) depicted continued cooling of the LSTs, primarily in the eastern basin where areas of 15°–17°C water developed. At deeper levels, the hindcasts showed a dramatic increase in the eastern basin dome along with a compression of metalimnion (Figs. 19d and 19f). The doming was less amplified in the forecasts due to an underestimation of the intensity of the eastern basin's counterclockwise gyre (not shown). The highly amplified dome in the hindcasts was likely responsible for

the appearance of the colder surface water in the eastern basin. The hindcasts also depicted an increase in the thickness of the epilimnion, an increase in the depth of the thermocline, and a warming of the hypolimnion. This was not seen in the forecasts.

Hourly LST forecasts were compared to observations at buoys 45132 and 45005 and platform 45134 (Fig. 20 and Table 3). At buoy 45132, the forecasts were warmer than observed while at buoy 45005 and platform 45134 the forecasts and hindcasts were generally cooler than the observations. The difference between simulations and observations at buoy 45005 and platform 45134 suggest a cold bias after the spinup period. However, a comparison of the forecasts to the hindcasts indicates
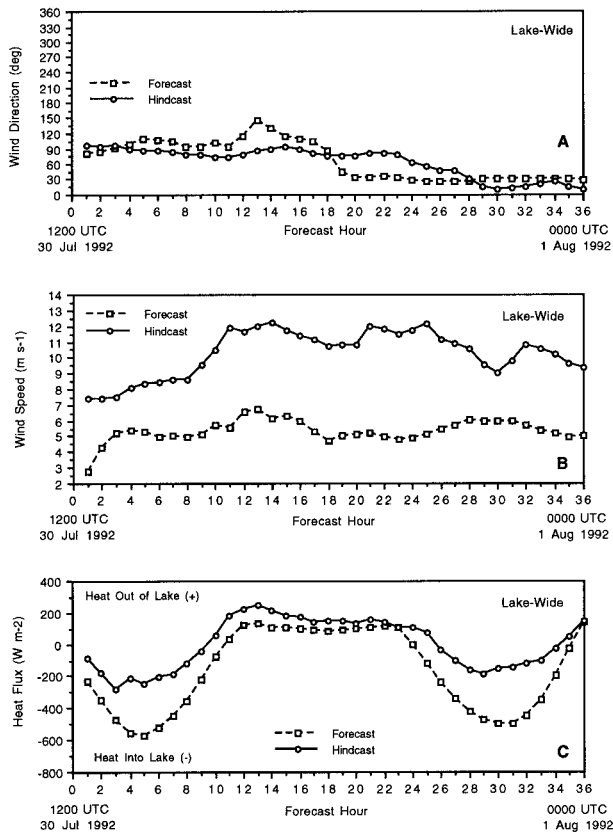
FIG. 16. Hourly lake-wide means of (a) wind direction (°), (b) wind speed (m s^{-1}), and (c) surface heat flux (W m^{-2}) from 1300 UTC 30 July to 0000 UTC 1 August 1992.
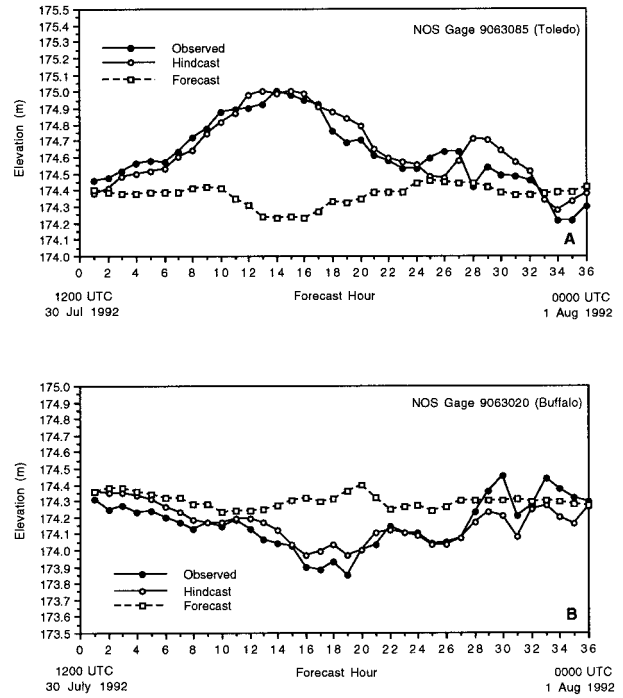

FIG. 17. Hourly forecast, hindcast, and observed water levels for NOS stations at (a) Toledo and (b) Buffalo from 1300 UTC 30 July to 0000 UTC 1 August 1992.

once again the effect of the MM4 model introducing excess heat into the lake. A comparison of the forecasts to climatology at buoy 45005 indicates that the forecasts provided a better estimate of observed conditions at this site.

8. Autumn case

The third case covered the period from 1200 UTC 16 October to 0000 UTC 18 October 1992. In this case, a surface cyclone passed northwest of the lake as it was progressing toward isothermal conditions. This cyclone track is typical of autumn storms with strong southwest winds in advance of the cyclone followed by a sudden shift to the northwest as its cold front passes across the lake.

a. Initial lake conditions

The lake's water surface at the beginning of the period exhibited a tilt with a rise of water levels in the eastern basin and a drawdown in the western basin (not shown). This tilt was in response to the strong southwesterly winds in advance of the cold front. The initial water temperature structure (Fig. 21) depicted a typical early

to midautumn condition in which stratification is confined to the bottom of the eastern basin (Mortimer 1987). LSTs ranged from 13° to 17°C over most of the lake.

b. Lake and atmospheric conditions

At 1200 UTC 16 October, a surface low was located over central Lake Huron with its cold front over the western basin (Fig. 22a). Overlake winds were 6.1–12.8 m s^{-1} with gusts to 16.3 m s^{-1}. The low intensified 7 mb during the next 6 h and moved northeastward to Georgian Bay with its associated cold front over the central basin (not shown). Behind the front, overlake winds were from the west or west-northwest at sustained speeds of 10.2–20.4 m s^{-1}. Between 1800 and 2000 UTC the cold front passed over the rest of the lake. Overlake air temperatures dropped by about 8.4°C and wind speeds increased to 12.8–20.4 m s^{-1}. By 0000 UTC 17 October, the low was south of James Bay with a central pressure of 989 mb with its cold front located in central New York (Fig. 22b). Strong west-southwest winds between 10.2 and 20.4 m s^{-1} were present over the lake. Winds remained at these speeds for the next 6 h, but began to veer to the northwest. It was during this period at 0200 UTC that the lowest water level was recorded at Toledo. The elevation was of 173.04 m, 0.46 m below datum. This low water level along with the high level at Buffalo 5 h earlier represented a setup of 2.33 m. By 1200 UTC winds over the lake had decreased to approximately 10 m s^{-1} (Fig. 22c). Overlake winds
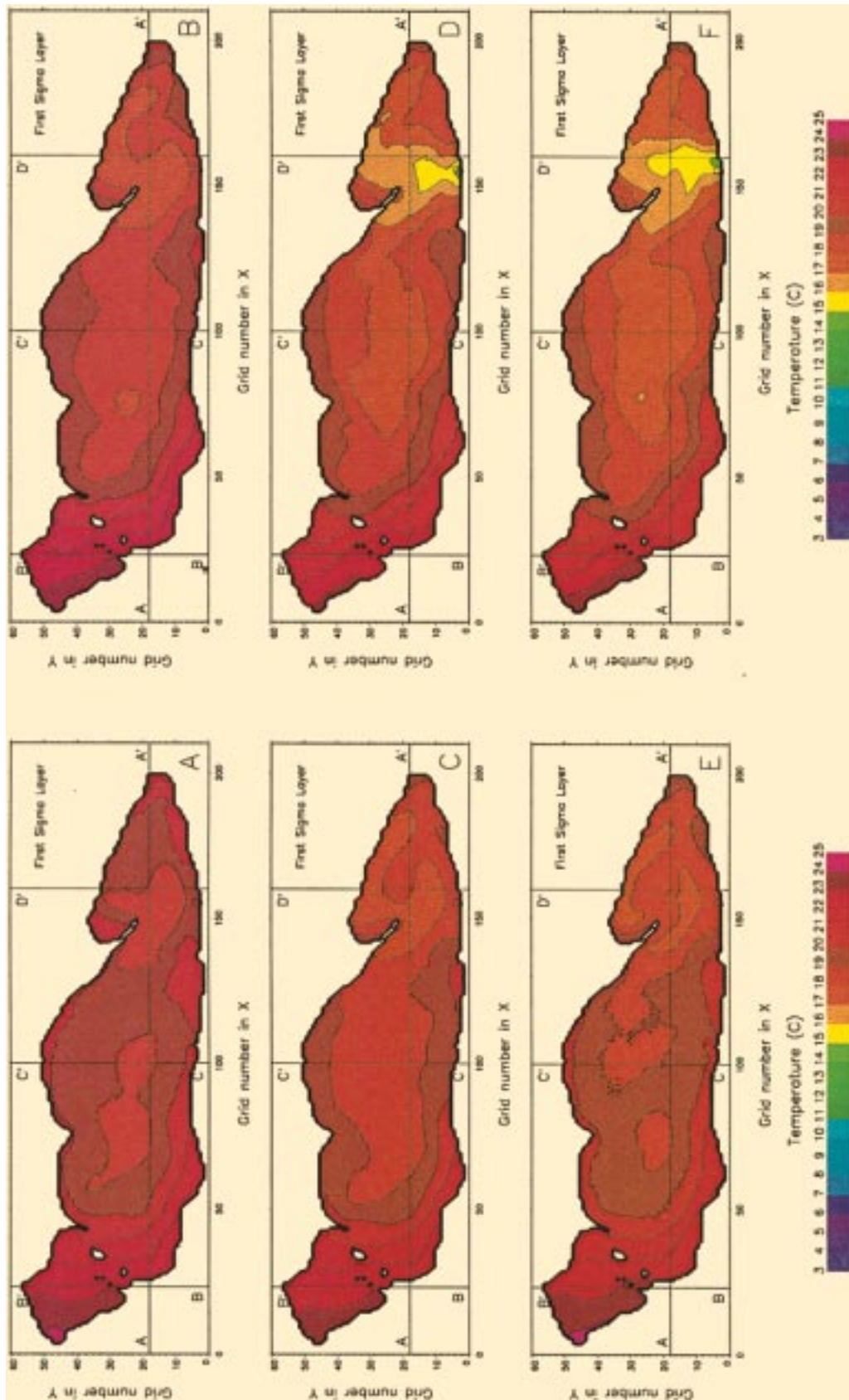
FIG. 18. LEIFS 12-, 24-, and 36-h surface water temperature forecasts for (a) 0000 UTC 31 July 1992, (c) 1200 UTC 31 July 1992, and (e) 0000 UTC 1 August 1992. Also shown are 12- (b), 24- (d), and 36-h (f) hindcasts for the same times. Contours are drawn at intervals of 1°C.
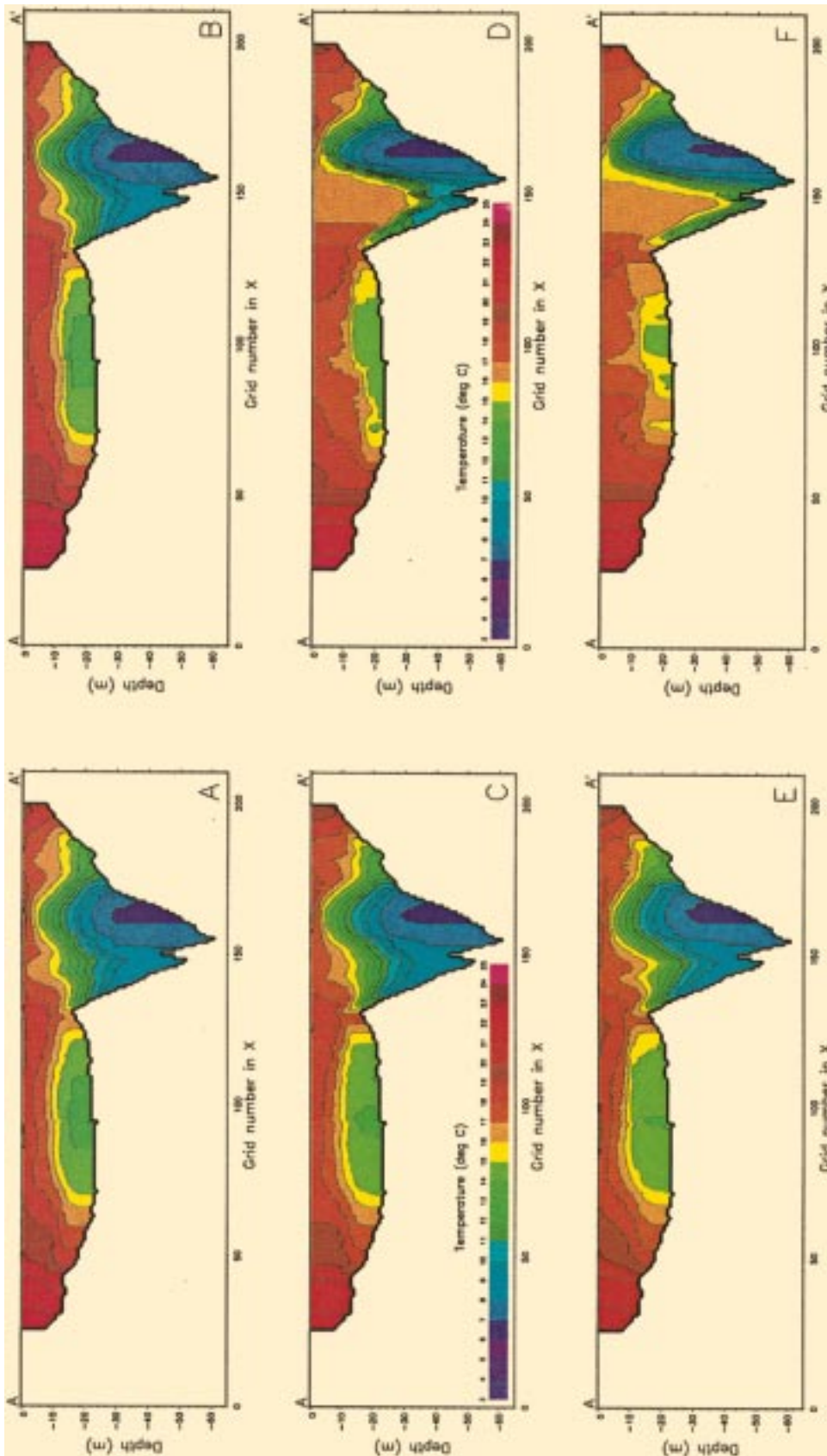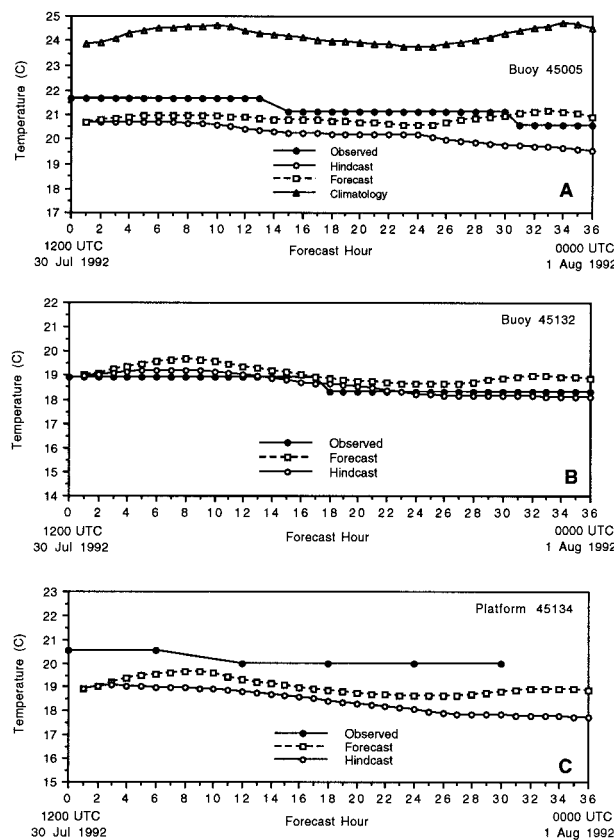
FIG. 19. LEIFS 12-, 24-, and 36-h subsurface water temperature forecasts as depicted in long-axis cross sections for (a) 0000 UTC 31 July 1992, (c) 1200 UTC 31 July 1992, and (e) 0000 UTC 1 August 1992. Also shown are 12- (b), 24- (d), and 36-h (f) hindcasts for the same times. Contours are drawn at intervals of 1°C.

FIG. 20. Forecast, hindcast, and observed surface water temperatures for (a) buoy 45132, (b) platform 45134, and (c) buoy 45005 for the period 1200 UTC 30 July to 0000 UTC 1 August 1992. A hourly climatology (12-yr mean) is also depicted for buoy 45005

gradually backed to the west and southwest as a high pressure area moved into the Midwest (Fig. 22d).

c. Atmospheric forecasts

Comparisons between the forecast (Fig. 23) and observed conditions indicate that MM4 did well in predicting the track, speed, and intensification of the surface cyclone and associated fronts through the Great Lakes region. It was also successful in predicting southwest winds over the lake in advance of the cold front and the shift to the northwest after the frontal passage. However, it was not as successful at predicting the shift back to southwest at the end of the forecast period (Fig. 24a). It also underestimated the strength of the prefrontal southwest winds. Forecast wind speeds were 2–4 m s^{-1} too low during the first 15 h and 2 m s^{-1} too low during the last 6 h (Fig. 24b). During the intervening 15 h, the forecasts overestimated the actual wind speeds by 2 m s^{-1}. For the entire 36-h period, the mean absolute difference between forecasts and observations was 2.3 m s^{-1}.

A comparison of total surface heat flux forecasts and hindcasts (Fig. 24c) indicates three different patterns. Heat

gain into the lake was overestimated from 100 to 400 W m^{-2} during the first 11 h of the forecast period. An examination of the individual components (not shown) revealed that the overprediction of heat into the lake was due to 1) an underprediction of the latent heat flux (i.e., too little heat out of the lake by evaporation) by 100–300 W m^{-2} and 2) an overprediction of shortwave radiation by 50–100 W m^{-2}. The underprediction of the latent heat flux was due an underestimation of wind speeds up to 6 m s^{-1}. The overprediction of the shortwave radiation was due to an underestimation of the cloud cover by 1–3 oktas. During the next 13 h, heat loss from the lake was overestimated by 200–300 W m^{-2} due to a positive bias of approximately 150 W m^{-2} in both the sensible and latent heat fluxes. The bias in the sensible heat flux was due to the surface temperature forecast being too cold (2°–3°C) and the wind speed forecasts being too large by 2 m s^{-1}. The positive bias in latent heat flux could be attributed primarily to the overprediction of surface wind speeds. During the last 7 h of the period, the forecasts and hindcasts were similar.

d. Lake forecasts

Forecasts of water levels called for an increase in the tilt up to 1200 UTC 17 October followed by a return to more spatially uniform conditions (not shown). Hindcasts depicted a more rapid increase in the tilt and subsequent return to uniform conditions. Comparisons of hourly water level forecasts to gauge observations indicate that the forecasts were fairly accurate over the period (Fig. 25). The forecasts were not so accurate in estimating the maximum and minimum observed water levels and their times of occurrence (Table 2). The maximum water level at Buffalo was underestimated by close to 0.5 m and lagged 6 h behind in the time of occurrence. The forecast of minimum water level at Toledo was underestimated by over 0.4 m. The time of minimum water level was off by 1 h. The poor performance is attributed to the MM4 underestimation of both the magnitude and timing of the southwesterly winds.

Both lake temperature forecasts and hindcasts for the first 12 h called for LSTs (Figs. 26a and 26b) and subsurface temperatures (Figs. 27a and 27b) to decrease slightly across the lake. However, the hindcast depicted a smaller area of remaining stratification in the eastern basin. The smaller areal extent was likely due to stronger vertical mixing caused by the higher winds than present in the forecasts. The hindcast showed a complete destruction of the eastern basin stratification by 1800 UTC (not shown). For the last 18 h, the model forecasts continued to decrease LSTs (Figs. 26c and 26e), especially in the western basin and along the central basin's shoreline. Below the surface, the stratification in the eastern basin was still present but smaller in area (Figs. 27c and 27e). Hindcasts (Figs. 27d and 27f) showed a similar cooling pattern as the forecasts but was different in the amount and areal extent of the cooling in the central
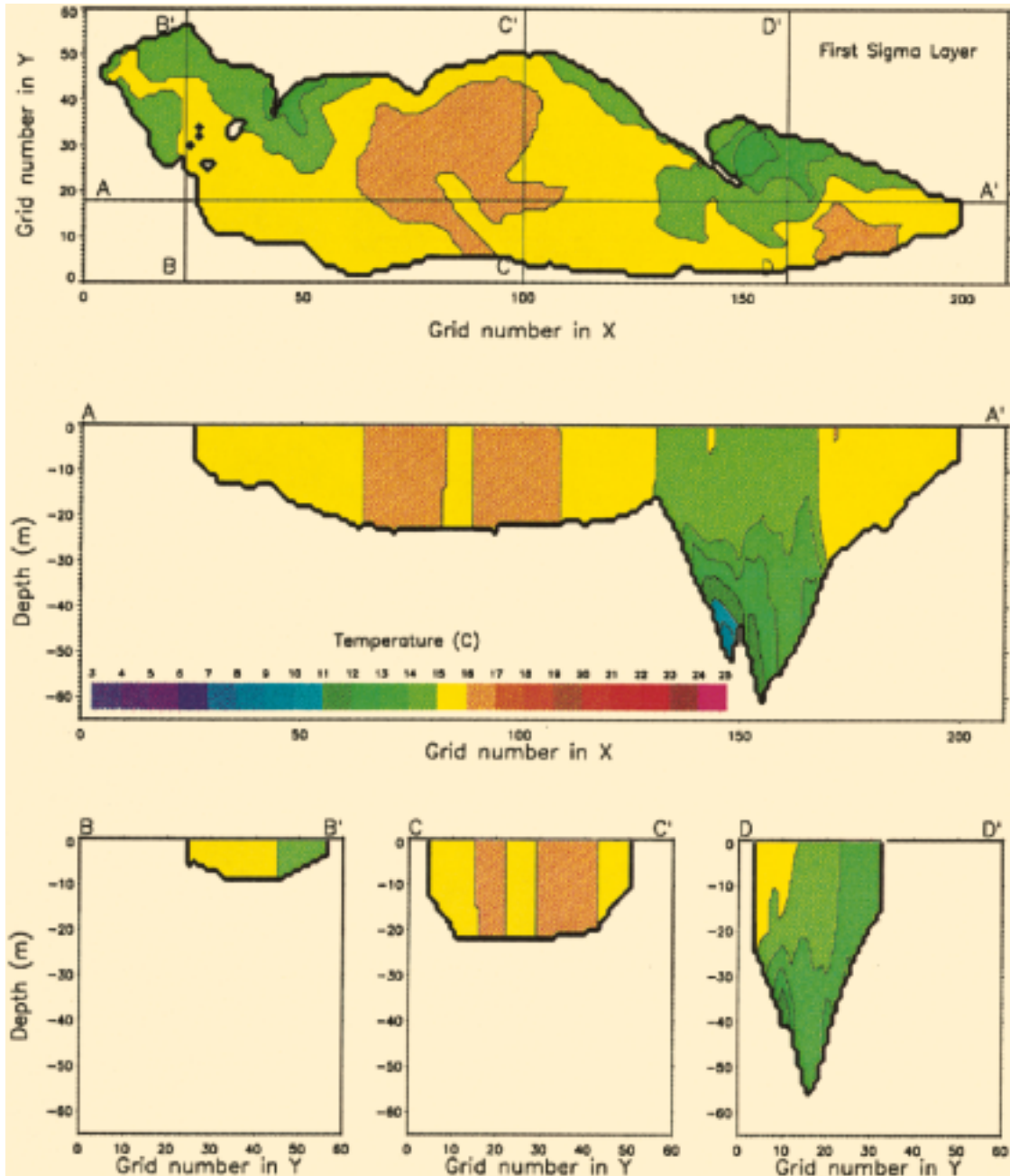
FIG. 21. LEIFS initial surface water temperatures along with long-axis and transverse vertical cross sections for 1200 UTC 16 October 1992.

basin. The hindcast depicted cooler water extending from the western basin into the central basin. This difference may have been the result of an eastward current induced by westerly winds, which developed near the end of the period. Comparisons between LST forecasts and in situ observations at buoy 45005 (Fig. 28a) indicate that the forecast and also the hindcasts started off with a cold bias of approximately 1°C. However, the forecasts correctly estimated the overall downward trend and were generally within 1°C of the observations. A comparison of the forecasts to climatology at buoy 45005 indicated that climatology was comparable to the forecasts but did not predict the overall downward trend (Table 3).

9. Summary

A one-way coupled atmosphere–lake modeling system was developed to generate short-term, mesoscale lake circulation, water level, and temperature forecasts
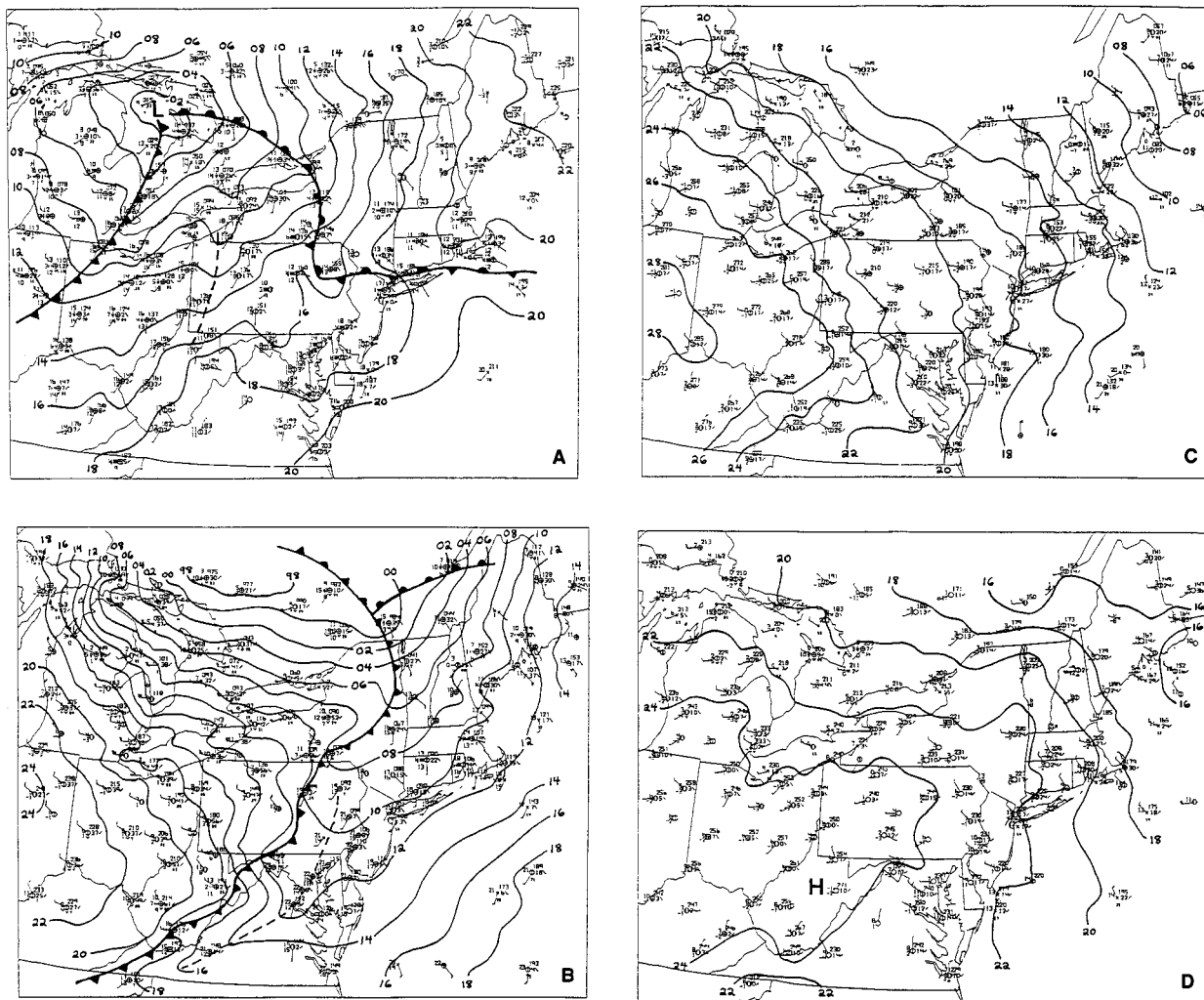
FIG. 22. Surface analyses at (a) 1200 UTC 16 October 1992, (b) 0000 UTC 17 October 1992, (c) 1200 UTC 17 October 1992, and (d) 0000 UTC 18 October 1992. Light solid lines are isobars (mb) plotted at an interval of 2 mb. Pressure troughs are noted by dashed lines.

for Lake Erie. The coupled system consisted of the semioperational versions of the Pennsylvania State University–National Center for Atmospheric Research hydrostatic, mesoscale meteorological model (MM4), and the lake circulation model of the Lake Erie Information Forecast System. The coupled system was evaluated in its ability to accurately forecast lake conditions 36 h in advance during severe lake conditions at three stages in the annual stratification cycle. These included the development stage ("fragile" stratification) in May, the mature stage (widespread stable stratification) in July, and the final decay stage (erosion of remaining stratification) in October. The lake forecasts were compared to both observations and hindcasts. In addition, the atmospheric forecasts used by the lake model were compared to observations.

The lake model did the worst in the prediction of water levels. The forecasts of the high and low water levels were off by 0.1 to 0.5 m in amplitude and from

9 h too early to 11 h too late in the timing of peak levels. These poor forecasts were related to the underestimation of the surface wind speeds and timing of wind direction shifts by MM4. Lake-wide mean algebraic differences between observed and MM4 wind forecasts indicated underestimated winds from approximately 1 to 5 m s^{-1}. Mean algebraic directional differences ranged from 4° to 22° indicating that the forecasts were generally clockwise of the observations.

In regard to the short-term prediction of the lake's thermal structure, the model captured the major changes in two of the cases. The lake model correctly forecast in the spring case the deepening of thermocline following a cold front passage with respect to both timing and final depth. It also predicted fairly well the autumn event when the last remaining area of stratification was eroded after a cold front passage. However, the model did not forecast as well the summertime event when dramatic changes occurred in the central and eastern basins. The
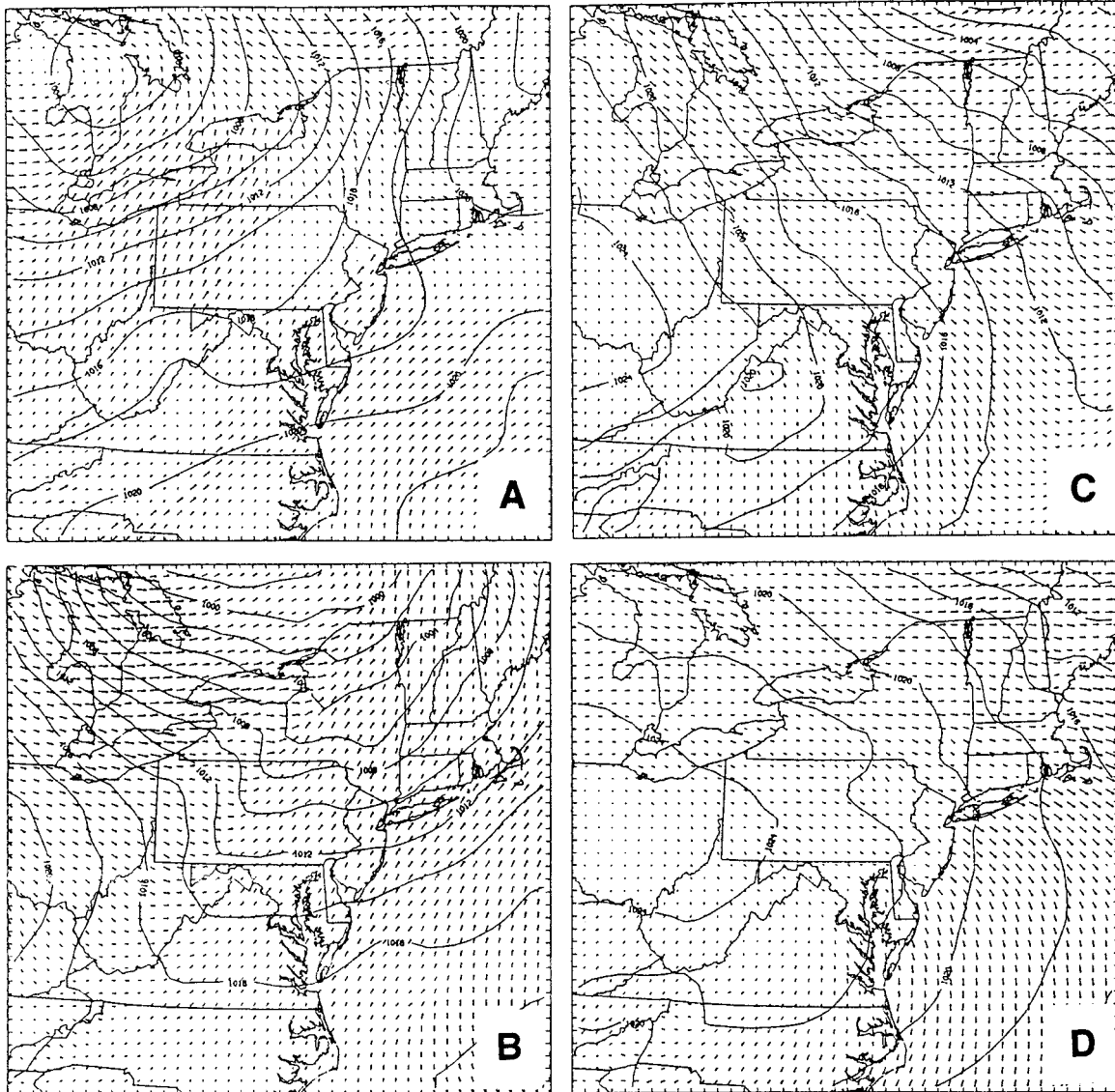
FIG. 23. MM4 fine-grid domain analysis and 12-, 24-, and 36-h forecasts of sea level pressure (mb) and surface (40 m AGL) winds (m s⁻¹) at (a) 1200 UTC 16 October 1992, (b) 0000 UTC 17 October 1992, (c) 1200 UTC 17 October 1992, and (d) 0000 UTC 18 October 1992. Light solid lines are isobars (mb) plotted at an interval of 2 mb.

forecasts pointed to a ''doming'' of the isotherms in the eastern basin but significantly underpredicted the amplitude of the dome. It also failed to forecast the change in the thickness of the epilimnion and hypolimnion. This case was marked by the greatest difference in lake-wide wind speeds between MM4 forecasts and observations. As noted earlier, MM4 wind forecasts were underestimated during the entire 36 h.

10. Conclusions

This study represents the first attempt to generate short-term forecasts of the three-dimensional physical structure of an inland water body using a one-way cou-

pled atmosphere–lake modeling system. Several conclusions can be made from this limited evaluation of the coupled system. First, a one-way coupled lake modeling system can be constructed using existing models and data sources. The operational implementation of such a system is now possible with the introduction of NCEP's Eta Mesoscale Model. The Eta Model has a horizontal resolution of 29 km (similar to MM4) with 50 layers in the vertical. The model is run twice a day and generates a 36-h forecast. Initial conditions for the lake model can be provided by the four times a day LEIFS nowcasts. Work has begun on using Eta Model forecasts for LEIFS (Hoch 1997).

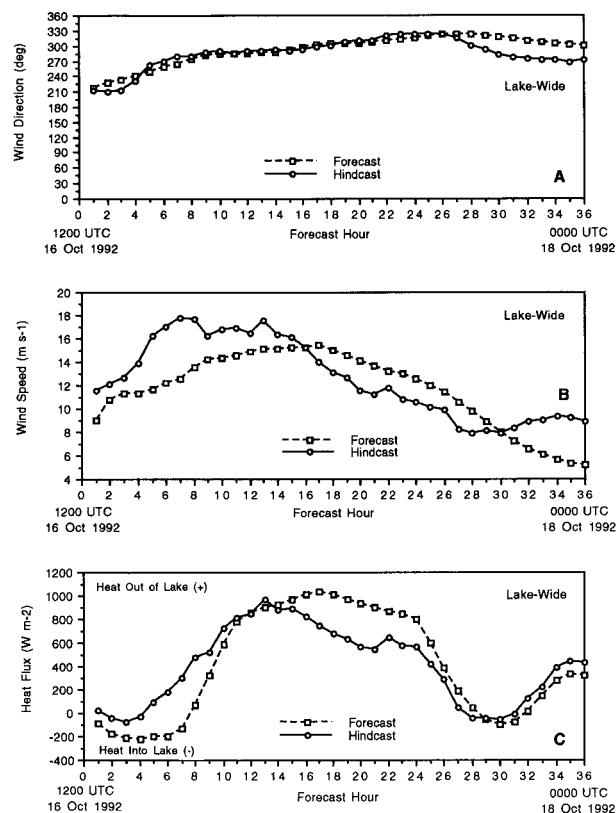A second conclusion was that the quality of the lake

FIG. 24. Hourly lake-wide means of (a) wind direction (°), (b) wind speed (m s⁻¹), and (c) surface heat flux (W m⁻²) from 1300 UTC 16 October to 0000 UTC 18 October 1992.
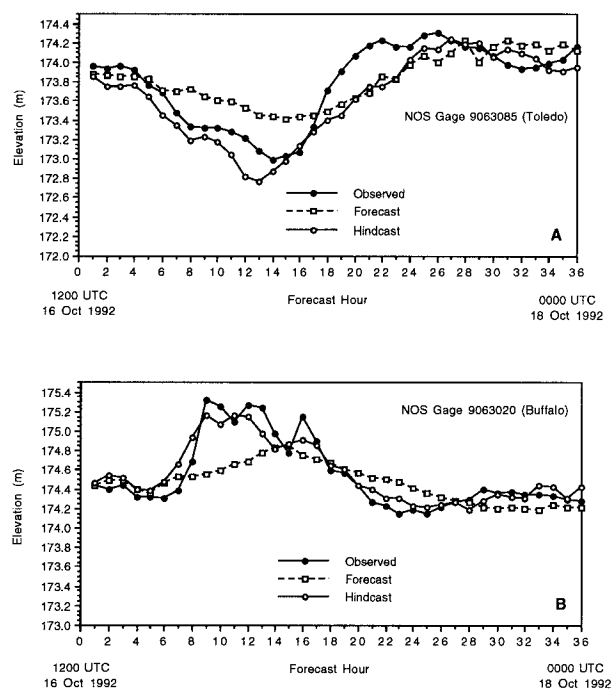

FIG. 25. Hourly forecast, hindcast, and observed water levels for NOS stations at (a) Toledo and (b) Buffalo from 1300 UTC 16 October to 0000 UTC 18 October 1992.

model forecasts were highly dependent on the atmospheric model forecasts, especially the wind conditions. This suggests the need for higher-resolution atmospheric models and more frequent atmospheric forecast updates to the lake models. Increases in the horizontal and vertical resolutions of NCEP operational atmospheric models are planned in the next few years. NCEP plans to test a 10-km version of the Eta Model over the Great Lakes region and to run a new 32-km version four times a day in 1998. Recently, the Canadian Meteorological Center ran in real time the Mesoscale Compressible Community (MC2) model to produce a 24-h forecast at 10-km resolution over the continental U.S. and Canada (Thomas et al. 1997). Other operational NCEP atmospheric modeling systems such as the Local Analysis Prediction System (Albers et al. 1996) and the new 40-km version of the Rapid Update Cycle (Benjamin et al. 1996) can provide the lake model with hourly surface meteorological nowcasts and frequent short-term forecasts. Frequent atmospheric model forecasts will be critical in accurately predicting the lake's rapid water level fluctuations.

Recent modeling studies including the one by Ljungemyr et al. (1996) have demonstrated the positive impact of parameterizing lake temperatures and lake-ice thickness in an operational atmospheric prediction model using a simple lake model. Similar parameterization of lake temperatures as well as wave height (roughness) conditions of the Great Lakes may be important in future operational mesoscale atmospheric models. Research has begun at NCAR in cooperation with Ohio State University and GLERL in the development of a two-way interactive coupled atmosphere–lake modeling system to examine air–lake interactions. The coupled system consists of the fifth-generation version of the Penn State–NCAR mesoscale meteorological model (Dudhia 1993) and the lake circulation and wave models used in LEIFS.
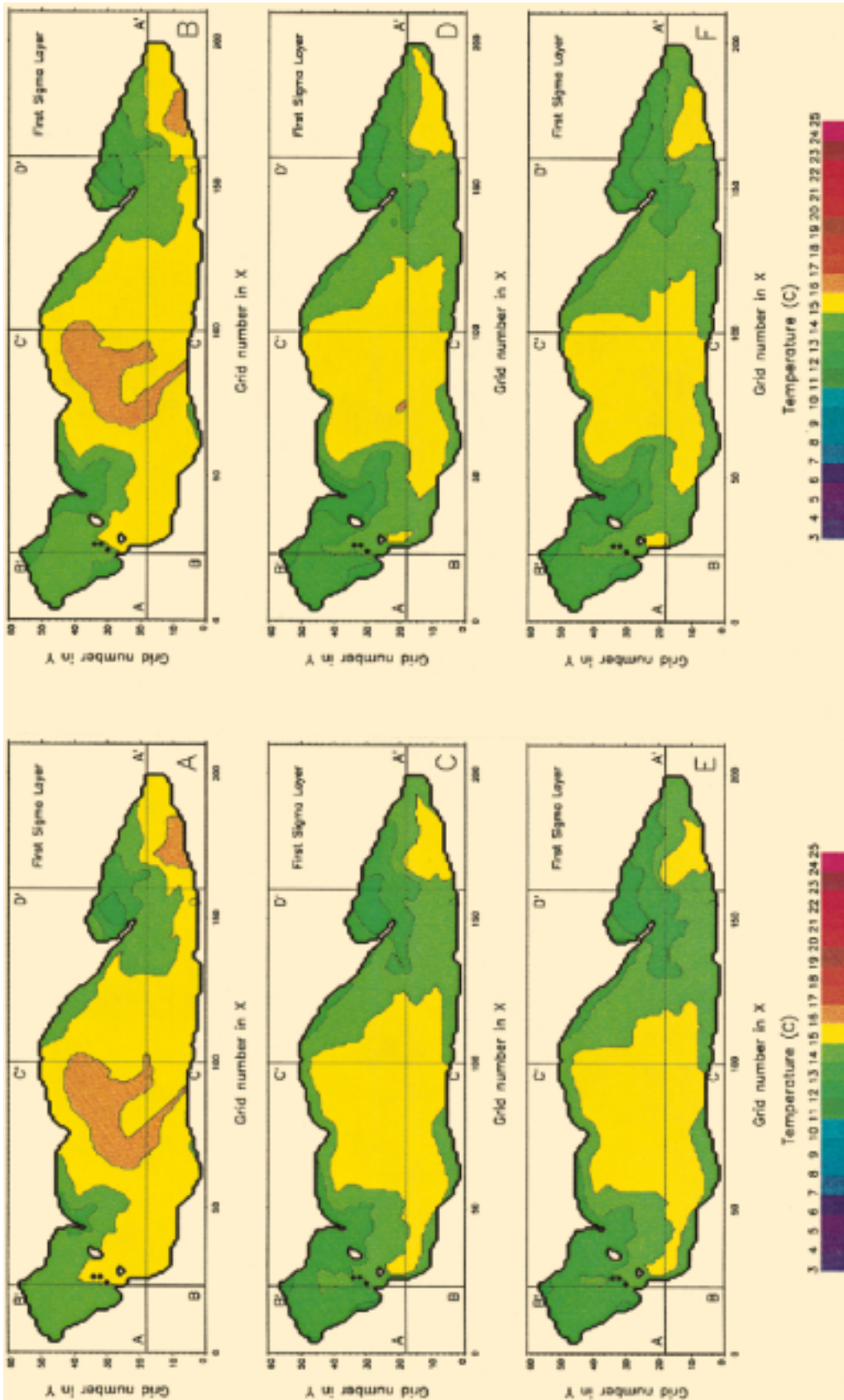
FIG. 26. LEIFS 12-, 24-, and 36-h surface water temperature forecasts for (a) 0000 UTC 17 October 1992, (c) 1200 UTC 17 October 1992, and (e) 0000 UTC 18 October 1992. Also shown are 12- (b), 24- (d), and 36-h (f) hindcasts for the same times. Contours are drawn at intervals of 1°C.
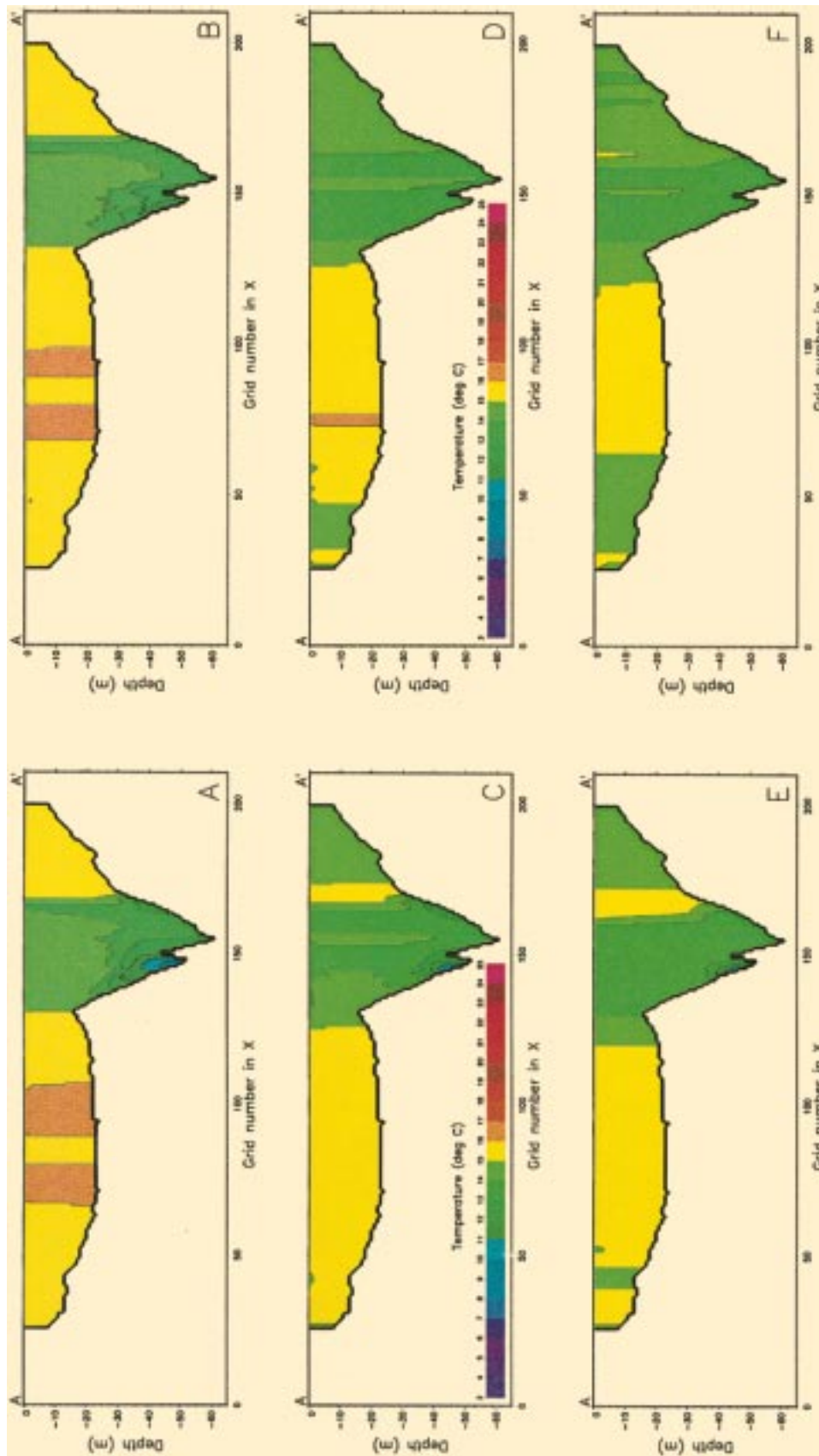
FIG. 27. LEIFS 12-, 24-, and 36-h subsurface water temperature forecasts as depicted in long-axis cross sections for (a) 0000 UTC 17 October 1992, (c) 1200 UTC 17 October 1992, and (e) 0000 UTC 18 October 1992. Also shown are 12- (b), 24- (d), and 36-h (f) hindcasts for the same times. Contours are drawn at intervals of 1°C.
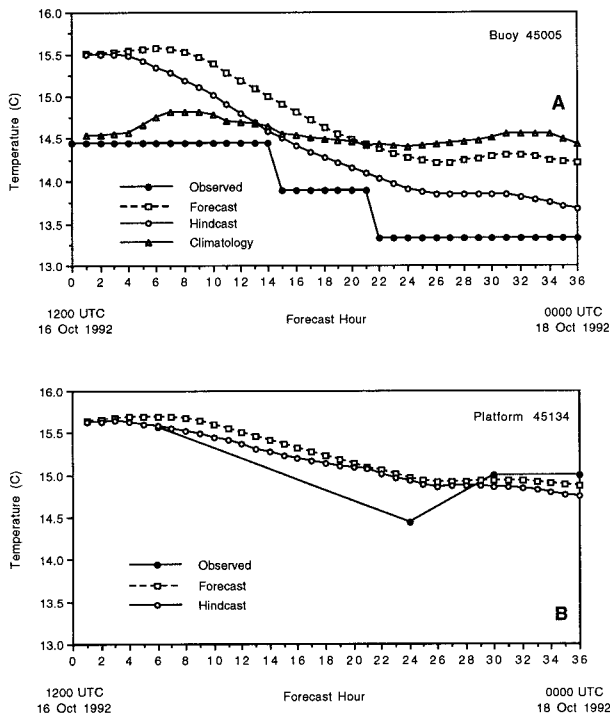
FIG. 28. Forecast, hindcast, and observed surface water temperatures for (a) buoy 45005 and (b) platform 45134 for the period 1200 UTC 16 October to 0000 UTC 18 October 1992. Observations were not available for buoy 45132.

REFERENCES

Albers, S. C., J. A. McGinley, D. L. Birkenheuer, and J. R. Smart, 1996: The Local Analysis and Prediction System (LAPS): Analyses of clouds, precipitation, and temperature. *Wea. Forecasting,* **11,** 273–287.

Anthes, R. A., 1990: Recent applications of the Penn State/NCAR mesoscale model in synoptic, mesoscale, and climate studies. *Bull. Amer. Meteor. Soc.,* **71,** 1610–1629.

——, and T. T. Warner, 1978: Development of hydrodynamic models suitable for air pollution and other meteorological studies. *Mon. Wea. Rev.,* **106,** 1045–1078.

——, E. Y. Hsie, and Y. H. Kuo, 1987: Description of the Penn State/NCAR Mesoscale Model Version 4 (MM4). NCAR Tech. Note 282+STR, NCAR, Boulder, CO, 66 pp.

Barnes, S. L., 1964: A technique for maximizing details in numerical weather map analysis. *J. Appl. Meteor.,* **3,** 396–409.

——, 1973: Mesoscale objective analysis using weighted time–series observations. NOAA Tech. Memo. ERL NSSL-62, National Severe Storms Laboratory, Norman, OK, 60 pp. [NTIS COM-73-10781.]

Bates, G. T., F. Giorgi, and S. W. Hostetler, 1993: Toward the simulation of the effects of the Great Lakes on regional climate. *Mon. Wea. Rev.,* **121,** 1373–1387.

Benjamin, S. G., J. M. Brown, K. J. Brundage, D. Devenyi, B. E. Schwartz, T. G. Smirnova, T. L. Smith, and F.-J. Wang, 1996: Recent upgrades to MAPS/RUC. FSL Forum, August, 1–11. [Available from NOAA Forecast System Laboratory, 325 Broadway, Boulder, CO, 80303-3328.]

Bennett, J. R., 1978: A three-dimensional model of Lake Ontario's summer circulation: II. A diagnostic study. *J. Phys. Oceanogr.,* **8,** 1095–1103.

Blackadar, A. K., 1976: Modeling the noctural boundary layer. Preprints, *Third Symp. on Atmospheric Turbulence, Diffusion and Air Quality,* Raleigh, NC, Amer. Meteor. Soc., 46–49.

——, 1979: High-resolution models of the planetary boundary layer. *Advances in Environmental Science and Engineering,* Vol. 1, J. R. Pfafflin and E. N. Ziegler, Eds., Gordon and Breach, Science Publishers, 50–85.

Blumberg, A. F., and G. L. Mellor, 1987: A description of a three-dimensional coastal ocean circulation model. *Three-Dimensional Coastal Ocean Models,* N. Heaps, Ed., Amer. Geophys. Union, 1–16.

Boyce, F. M., M. A. Donelan, P. F. Hamblin, C. R. Murthy, and T. J. Simons, 1989: Thermal structure and circulation in the Great Lakes. *Atmos.–Ocean,* **27,** 607–642.

Byrd, G. P., and R. S. Penc, 1992: The Lake Ontario snow event of 11–14 January 1990. Preprints, *Fifth Conf. on Mesoscale Processes,* Atlanta, GA, Amer. Meteor. Soc., J59–J66.

Changnon, S., Jr., and D. M. A. Jones, 1972: Reviews of the influences of the Great Lakes on weather. *Water Resour. Res.,* **8,** 360–371.

DeYoung, B., and C. L. Tang, 1989: An analysis of Fleet Numerical Oceanographic Center winds on the Grand Banks. *Atmos.–Ocean,* **27,** 414–427.

Dingman, J. S., and K. W. Bedford, 1986: Skill tests and parametric statistics for model evaluation. *J. Hydraul. Eng.,* **112,** 124–141.

Dudhia, J., 1993: A nonhydrostatic version of the Penn State–NCAR mesoscale model: Validation tests and simulation of an Atlantic cyclone and cold front. *Mon. Wea. Rev.,* **121,** 1493–1513.

Eichenlaub, V. L., 1979: *Weather and Climate of the Great Lakes Region.* University of Notre Dame, 355 pp.

Gilhousen, D. B., 1987: A field evaluation of NDBC moored buoy winds. *J. Atmos. Oceanic Technol.,* **4,** 94–104.

Hass, H., M. Memmesheimer, H. Geib, H. J. Jakobs, M. Laube, and A. Ebel, 1990: Simulation of the Chernobyl radioactive cloud over Europe using the EURAD model. *Atmos. Environ.,* **24A,** 673–692.

Hoch, B., 1997: An evaluation of a one-way coupled atmosphere–lake model for Lake Erie. M.S. thesis, Atmospheric Sciences Program, Ohio State University, 226 pp. [Available from Atmospheric Sciences Program, 1049 Derby Hall, 154 N. Oval Mall, Ohio State University, Columbus, OH 43210-1361.]

Hoke, J. E., N. A. Phillips, G. J. DiMego, J. J. Tuccillo, and J. G. Sela, 1989: The Regional Analysis and Forecast System of the National Meteorological Center. *Wea. Forecasting,* **4,** 323–334.

Kelley, J. G. W., 1995: One-way coupled atmospheric–lake model forecasts for Lake Erie. Ph.D. dissertation, Ohio State University, 450 pp. [Available from Atmospheric Sciences Program, 1049 Derby Hall, 154 N. Oval Mall, Ohio State University, Columbus, OH 43210-1361.]

Koch, S. E., M. DesJardins, and P. J. Kocin, 1983: An interactive Barnes objective map analysis scheme for use with satellite and conventional data. *J. Climate Appl. Meteor.,* **22,** 1487–1503.

Kuan, C.-F., 1995: Performance evaluation of the Princeton Circulation Model for Lake Erie. Ph.D. dissertation, Ohio State University, 376 pp. [Available from Dept. of Civil and Environmental Engineering and Geodetic Science, 470 Hitchcock Hall, 2070 Neil Ave., Ohio State University, Columbus, OH 43210-1275.]

Liu, P. C., and D. J. Schwab, 1987: A comparison of methods for estimating u* from a given u_z and air–sea temperature differences. *J. Geophys. Res.,* **92,** 6488–6494.

Ljungemyr, P., N. Gustafsson, and A. Omstedt, 1996: Parameterization of lake thermodynamics in a high-resolution weather forecasting model. *Tellus,* **48A,** 608–621.

Lyons, W. A., 1971: Low level divergence and subsidence over the Great Lakes in summer. *Proc. 14th Conf. on Great Lakes Research,* Toronto, ON, Canada, Int. Association of Great Lakes Research, 467–486.

McCormick, M. J., and G. A. Meadows, 1988: An intercomparison

of four mixed layer models in a shallow inland sea. *J. Geophys. Res.,* **93,** 6774–6788.

Mellor, G. L., 1996: Users guide for a three-dimensional, primitive equation, numerical ocean model. Program in Atmospheric and Oceanic Sciences, Princeton University, Princeton, NJ, 39 pp. [Available from Program in Atmospheric and Oceanic Sciences, P.O. Box CN710, Sayre Hall, Princeton University, Princeton, NJ 08544-0710.]

Mortimer, C. H., 1987: Fifty years of physical investigations and related limnological studies on Lake Erie, 1928–1977. *J. Great Lakes Res.,* **13,** 407–435.

NRC, 1989: Opportunities to improve marine forecasting. Committee on Opportunities to Improve Marine Observations and Forecasting, Marine Board, Commission on Engineering and Technical Systems, National Research Council, Washington, DC, 125 pp. [Available from National Research Council, 2101 Constitution Avenue, Washington, DC 20418.]

O'Connor, W. P., and D. J. Schwab, 1993: Sensitivity of Great Lakes Forecasting System nowcasts to meteorological fields and model parameters. *Proc. ASCE Third Int. Conf. on Estuarine and Coastal Modeling,* Oak Brook, IL, Amer. Soc. Civil Eng., 149–157.

Phillips, D. W., and J. G. Irbe, 1978: Lake to land comparison of wind, temperature, and humidity on Lake Ontario during the International Field Year for the Great Lakes (IFYGL). Atmospheric Environment Service Rep. CLI-2-77, 51 pp. [Available from Atmospheric Environment Service, 4905 Dufferin St., Downsview, ON M3H 5T4 Canada.]

Resio, D. T., and C. L. Vincent, 1977: Estimation of winds over the Great Lakes. *J. Waterways, Port, Coast, Ocean Div.,* **103,** 265–283.

Rew, J., 1992: STORM-FEST: Real-time mesoscale modeling begins. *NCAR Scientific Comput. Div. News,* **13,** 3–5.

Ricketts, J. N., 1973: An investigation into a relationship between upper-air relative humidity and cloud cover. *Meteor. Mag.,* **102,** 146–153.

Schertzer, W. M., J. H. Saylor, F. M. Boyce, D. G. Robertson, and F. Rosa, 1987: Seasonal thermal cycle of Lake Erie. *J. Great Lakes Res.,* **13,** 468–486.

Schwab, D. J., 1978: Simulation and forecasting of Lake Erie storm surges. *Mon. Wea. Rev.,* **106,** 1476–1477.

——, 1983: Numerical simulation of low-frequency current fluctuations in Lake Michigan. *J. Phys. Oceanogr.,* **13,** 2213–2224.

——, and D. L. Sellers, 1980: Computerized bathymetry and shorelines. NOAA Data Rep. ERL GLERL-16, Great Lakes Environmental Research Laboratory, Ann Arbor, MI, 13 pp. [Available from NOAA/Great Lakes Environmental Research Laboratory, Publications Office, 2205 Commonwealth Blvd., Ann Arbor, MI 48105-2945.]

——, and K. W. Bedford, 1994: Initial implementation of the Great Lakes Forecasting System: A real-time system for predicting lake circulation and thermal structure. *Water Pollut. Res. J. Can.,* **29,** 203–220.

——, M. A. Donelan, J. R. Bennett, and P. C. Liu, 1984: Application of a simple numerical wave prediction model to Lake Erie. *J. Geophys. Res.,* **89,** 3586–3592.

——, W. P. O'Connor, and G. L. Mellor, 1995: On the net cyclonic circulation in large stratified lakes. *J. Phys. Oceanogr.,* **25,** 1516–1520.

Simons, T. J., 1976: Verification of numerical models of Lake Ontario: III. Long-term heat transports. *J. Phys. Oceanogr.,* **6,** 372–378.

Sousounis, P. J., and J. M. Fritsch, 1994: Lake-aggregate mesoscale disturbances. Part II: A case study of the effects on regional and synoptic-scale weather systems. *Bull. Amer. Meteor. Soc.,* **75,** 1793–1811.

Strub, P. T., and C. James, 1990: Evaluation of surface wind fields over the coastal ocean off the western U.S. *Rep. of the Planning Workshop for the Coastal Ocean Prediction Systems Program: Understanding and Managing Our Coastal Ocean, Vol. II: Overview and Invited Papers,* New Orleans, LA, Joint Oceanographic Institutions, 146–165. [Available from Joint Oceanographic Institutions, Inc., 1775 Massachusetts Ave., NW, Suite 800, Washington, DC 20036-2102.]

Sullivan, D. J., 1988: Objective temperature prediction by cloudiness using the Model Output Enhancement Technique. M.S. thesis, Dept. of Horticulture, The Pennsylvania State University, 134 pp. [Available from Dept. of Horticulture, 101 Tyson Building, The Pennsylvania State University, University Park, PA 16802.]

Thomas, S., R. Benoit, and M. Desgagne, 1997: News flash. *CMOS Bull.,* **25,** 102–103.

Thompson, E. F., and D. A. Leenknecht, 1994: Wind estimation for coastal modeling applications. *J. Coastal Res.,* **10,** 628–636.

Warner, T. T., and N. L. Seaman, 1990: A real-time, mesoscale numerical weather-prediction system used for research, teaching, and public service at The Pennsylvania State University. *Bull. Amer. Meteor. Soc.,* **71,** 792–805.

——, D. F. Kibler, and R. L. Steinhart, 1991: Separate and coupled testing of meteorological and hydrological forecast models for the Susquehanna River basin in Pennsylvania. *J. Appl. Meteor.,* **30,** 1521–1533.

Wetzel, R. G., 1983: *Limnology.* Saunders College Publishing, 767 pp.

Willmott, C. J., 1982: Some comments on the evaluation of model performance. *Bull. Amer. Meteor. Soc.,* **63,** 1309–1313.

——, 1984: On the evaluation of model performance in physical geography. *Spatial Statistics and Models,* G. L. Gaile and C. J. Willmott, Eds., Reidel Publishing, 443–460.

Yen, C.-C. J., J. G. W. Kelley, and K. W. Bedford, 1994: Daily procedure for GLFS nowcasts. *Proc. National Conf. on Hydraulic Engineering,* Buffalo, NY, Amer. Soc. Civil Eng., 202–206.

Zhang, D., and R. A. Anthes, 1982: A high-resolution model of the planetary boundary layer—Sensitivity tests and comparisons with SESAME-79 data. *J. Appl. Meteor.,* **21,** 1594–1609.